

# Thermodynamics of self-gravitating systems

Pierre-Henri Chavanis<sup>1,2</sup>, Carole Rosier<sup>3</sup> and Clément Sire<sup>1</sup>

<sup>1</sup> Laboratoire de Physique Quantique UMR CNRS 5626, Université Paul Sabatier,  
118 route de Narbonne 31062 Toulouse, France.

<sup>2</sup> Institute for Theoretical Physics, University of California, Santa Barbara, California.

<sup>3</sup> UMR CNRS 5585, Analyse Numérique, Université Lyon 1, bât. 101,  
69622 Villeurbanne Cedex, France.

## Abstract

Self-gravitating systems are expected to reach a statistical equilibrium state either through collisional relaxation or violent collisionless relaxation. However, a maximum entropy state does not always exist and the system may undergo a “gravothermal catastrophe”: it can achieve ever increasing values of entropy by developing a dense and hot “core” surrounded by a low density “halo”. In this paper, we study the phase transition between “equilibrium” states and “collapsed” states with the aid of a simple relaxation equation [Chavanis, Sommeria and Robert, *Astrophys. J.* **471**, 385 (1996)] constructed so as to increase entropy with an optimal rate while conserving mass and energy. With this numerical algorithm, we can cover the whole bifurcation diagram in parameter space and check, by an independent method, the stability limits of Katz [Mon. Not. R. astr. Soc. **183**, 765 (1978)] and Padmanabhan [*Astrophys. J. Supp.* **71**, 651 (1989)]. When no equilibrium state exists, our relaxation equation develops a self-similar collapse leading to a finite time singularity.

## 1 Introduction

It is fascinating to realize that galaxies follow a kind of organization revealed in the Hubble classification or in de Vaucouleurs’  $R^{1/4}$  law for the surface brightness of ellipticals [1]. The question that naturally emerges is, what determines the particular configuration to which a galaxy settles. It is possible that their present configuration depends crucially on the conditions that prevail at their birth and on the details of their evolution. However, in view of their apparent regularity, it is tempting to investigate whether their organization can be favored by some fundamental physical principles like those of thermodynamics and statistical physics. We ask therefore whether the actual states of galaxies (or self-gravitating systems in general) are not simply more probable than any other possible configuration, i.e. whether they can be considered as maximum entropy states. This approach may be particularly relevant for elliptical galaxies and globular clusters that are described by a distribution function that is almost isothermal [1]. In the case of elliptical galaxies, the evolution is collisionless (described by the Vlasov equation) but these systems are expected to reach a maximum entropy state on a few dynamical times  $t_D$  as a result of a “violent relaxation” [2, 3, 4, 5, 6, 7]. In the case of globular clusters, the relaxation proceeds via two-body encounters (on a relaxation time  $t_R \gg t_D$ ) and this collisional evolution is well-described by kinetic equations of a Fokker-Planck-Landau type for which a  $H$ -theorem is available [8, 9].

The statistical mechanics of stellar systems turns out to be very different from that of other, more familiar, many-body systems like neutral gases and plasmas due to the unshielded, long range nature of the gravitational force. Because of this fundamental difference, the statistical mechanics of self-gravitating systems encounters some problems, as the notion of equilibrium is not always well-defined [9, 10]. In section 2, we discuss the existence (or non existence !) of entropy maxima. These results are well-known [9], but we provide new and rigorous proofs based on a precise physical picture. In subsection 2.1, we introduce a mean-field description of the system and show that critical points of entropy at fixed energy  $E$  and mass  $M$  correspond to isothermal spheres like those studied in the context of stellar structure [11]. In section 2.2, we recall the particularity of self-gravitating systems to have negative specific heats. In subsection 2.3, we show that there is no global entropy maximum in an unbounded domain: a self-gravitating system can always increase entropy by taking a “core-halo” structure and spreading its density. In subsection 2.4, we show that there is not even a local entropy maximum in an unbounded domain: isothermal spheres have an infinite mass ! We restrict therefore our analysis to the case of stellar systems confined to a spherical box of radius  $R$  against which the stars bounce elastically (Antonov problem [12]). In subsection 2.5, we show that there is no *global* entropy maximum in a box: the system can always increase entropy by developing a dense and hot “core” surrounded by a low density “halo”. There exists, however, *local* entropy maxima (subsection 2.6) if the parameter  $\Lambda = -ER/GM^2$ , where  $G$  is the gravity constant, is less than  $\Lambda_c = 0.3345\dots$  and the density contrast  $\mathcal{R} = \rho(0)/\rho(R) \lesssim 709$ . Critical points of entropy with density contrast  $\mathcal{R} \gtrsim 709$  are unstable saddle points. For  $\Lambda > \Lambda_c$ , there are not even critical points of entropy. In that case, the system is expected to collapse and overheat; this is called the “gravothermal catastrophe” or “Antonov instability” [13]. In the case of globular clusters the collapse is halted and reversed due to the formation of binaries [14, 15]. In the case of collisionless stellar systems, or for self-gravitating fermions, the core ceases to shrink when it becomes degenerate (section 2.8). In that case, the system falls on to a global entropy maximum; it has a “core-halo” structure with a degenerate core and a low density halo, as calculated by Chavanis & Sommeria [5].

In section 3, we propose a numerical check of Antonov instability based on a simple relaxation equation introduced by Chavanis *et al.* [4, 3, 7]. This equation is constructed so as to increase entropy with an optimal rate while conserving exactly the total mass and the total energy of the system. It was shown by Rosier [16] that this equation is mathematically well-posed and that it possesses natural physical properties. It provides therefore an interesting model to study the phase transitions between “equilibrium” states and “collapsed” states depending on the value of the control parameter  $\Lambda$ . In subsection 3.1, we interpret our relaxation equation as a Smoluchowski equation coupled to gravity via a Poisson equation. In subsection 3.2, we derive the relaxation equation from a Maximum Entropy Production Principle and list its main properties. In subsection 3.3, we perform a linear stability analysis of this equation. We show that a stationary solution is linearly stable if and only if it is a local entropy maximum (Appendix C) and that the eigenvalue problem for linear stability is connected to the eigenvalue problem for the second order variations of entropy studied by Padmanabhan [17]. In section 4, we consider the case of gravitational collapse and look for self-similar solutions of our relaxation equation. Since the system is confined within a box, there is a small deviation to the purely self-similar solution and we describe this effect in detail.

In section 5, we perform various numerical simulations for different initial conditions. We confirm the findings of Antonov [12], namely the convergence towards an equilibrium state for  $\Lambda < \Lambda_c$  and the gravitational collapse for  $\Lambda > \Lambda_c$ . We find that the collapse proceeds self-similarly with explosion, in a finite time  $t_{coll}$ , of the central density, temperature and entropy while the core radius shrinks to zero. In the limit  $t \rightarrow t_{coll}$ , we find the scaling laws  $\rho_0 r_0^\alpha \sim 1$  and

$\rho/\rho_0 \sim (r/r_0)^{-\alpha}$  with  $\alpha \simeq 2.21$  in good agreement with our theoretical prediction of section 4. The collapse time diverges like  $t_{coll} \sim (\Lambda - \Lambda_c)^{-1/2}$  as we approach the critical point  $\Lambda_c$ . We also study the linear development of the instability (for unstable isothermal spheres) and show that the density perturbation  $\delta\rho/\rho$  presents several oscillations depending on the value of the density contrast. In particular, for the critical value  $\mathcal{R} \simeq 709$ , which corresponds to marginal stability ( $\Lambda = \Lambda_c$ ), the perturbation  $\delta\rho/\rho$  has a “core-halo” structure in agreement with Padmanabhan’s analysis [17]. We have also considered the situation in which the temperature  $T = 1/\beta$  is fixed instead of the energy  $E$ . In that case, the system can be in statistical equilibrium only if  $\eta \equiv \beta GM/R < \eta_c$  with  $\eta_c = 2.517\dots$  and  $\mathcal{R} \lesssim 32.1$ . For  $\eta > \eta_c$ , one observes gravitational collapse and our relaxation equation displays a self-similar behavior with an exponent  $\alpha = 2$ . In that case, the invariant profile  $\rho/\rho_0 = f(r/r_0)$  can be determined analytically. We also find that the collapse time behaves like  $t_{coll} \sim (\eta - \eta_c)^{-1/2}$  near the critical point. The perturbation  $\delta\rho/\rho$  that induces instability at the critical point does *not* present a “core-halo” structure in agreement with the thermodynamical analysis of Chavanis [18] in the canonical ensemble.

On a qualitative level, the first part of the paper (sections 2.1-2.7) is formulated in the context of the collisional relaxation of stellar systems in which heat transfers between core and halo play a prevalent role, while the second part of the paper (sections 2.8-5) is more adapted to the concept of “violent relaxation” as it focuses on the dynamical relaxation of stellar systems initially far from mechanical equilibrium. Of course, on a formal point of view the problem is to maximize an entropy functional at fixed mass and energy and this mathematical problem is common to both collisional and collisionless relaxation.

## 2 Statistical mechanics of stellar systems

### 2.1 The Maximum Entropy Principle

Consider a system of  $N$  stars, each of mass  $m$ , interacting via Newtonian gravity. We assume that the system is isolated so that the evolution conserves the energy  $E$  and the total mass  $M = Nm$ . Let  $f(\mathbf{r}, \mathbf{v}, t)$  denote the distribution function of the stellar system, i.e.  $f(\mathbf{r}, \mathbf{v}, t) d^3\mathbf{r} d^3\mathbf{v}$  gives the mass of stars whose position and velocity are in the cell  $(\mathbf{r}, \mathbf{v}; \mathbf{r} + d^3\mathbf{r}, \mathbf{v} + d^3\mathbf{v})$  at time  $t$ . The integral of  $f$  over the velocity determines the star density

$$(1) \quad \rho = \int f d^3\mathbf{v}.$$

In a mean-field approximation, the total mass and the total energy of the system are given by

$$(2) \quad M = \int \rho d^3\mathbf{r},$$

$$(3) \quad E = \frac{1}{2} \int f v^2 d^3\mathbf{r} d^3\mathbf{v} + \frac{1}{2} \int \rho \Phi d^3\mathbf{r} = K + W,$$

where  $K$  is the kinetic energy and  $W$  the potential energy. The gravitational potential  $\Phi$  is related to the star density by the Newton-Poisson equation

$$(4) \quad \Delta\Phi = 4\pi G\rho.$$

We ask which configuration maximizes the Boltzmann entropy

$$(5) \quad S = - \int f \ln f d^3\mathbf{r} d^3\mathbf{v},$$

subject to the conservation of mass and energy. Introducing Lagrange multipliers and writing the variational principle in the form

$$(6) \quad \delta S - \beta \delta E - \alpha \delta M = 0,$$

we find that the first order variations of the constrained entropy vanish for the Maxwell-Boltzmann distribution

$$(7) \quad f = A' e^{-\beta(\frac{v^2}{2} + \Phi)},$$

where the gravitational potential  $\Phi$  appears explicitly. The stellar density is simply obtained by integrating Eq. (7) over the velocities yielding

$$(8) \quad \rho = A e^{-\beta \Phi}, \quad A = \left(\frac{2\pi}{\beta}\right)^{3/2} A'.$$

According to Eq. (6), the Maxwell-Boltzmann distribution (7) is a *critical* point of entropy. This does not insure, however, that it is an entropy *maximum*. It is not even clear that the extremum problem (6) has a solution. Indeed, the gravitational potential that appears in Eq. (7) must be determined self-consistently by solving the mean field equation

$$(9) \quad \Delta \Phi = 4\pi G A e^{-\beta \Phi},$$

obtained by substituting the density (8) in the Poisson equation (4), and relating the Lagrange multipliers  $A, \beta$  to the constraints  $M, E$ . As we shall see, this problem does not always have a solution. When a solution exists, we must consider the second order variations of entropy  $\delta^2 S$  to determine whether it is an entropy maximum or not. Before considering this problem in detail, we show that self-gravitating systems display negative specific heats. This will help us developing a physical intuition of the direction of heat transfers in stellar systems (e.g., globular clusters) and understanding the physical origin of their instabilities.

## 2.2 Negative specific heats

When the distribution function  $f$  is given by the Maxwell-Boltzmann statistics (7), the kinetic energy of the system can be written

$$(10) \quad K = \frac{3}{2} M T.$$

where  $T = 1/\beta$  is the temperature. On the other hand, according to the Virial theorem [1], the potential energy of a self-gravitating system at equilibrium is related to its kinetic energy by

$$(11) \quad 2K + W = 0.$$

Therefore, the total energy  $E = K + W$  can be written equivalently

$$(12) \quad E = -K = \frac{1}{2} W.$$

It is opposite to the kinetic energy and equal to half the potential energy. Combining equations (10) and (12), we get

$$(13) \quad E = -\frac{3}{2} M T.$$

We find therefore that self-gravitating systems have negative specific heats [13]:

$$(14) \quad C \equiv \frac{dE}{dT} = -\frac{3}{2} M < 0.$$

By losing energy, their core automatically gets hotter and shrinks ! Because of this strange property, a self-gravitating system can never be in a true thermodynamical equilibrium state.

## 2.3 Absence of global entropy maximum in an unbounded domain

**Theorem 1:** There is no global entropy maximum in an unbounded domain. A self-gravitating system can always increase entropy by taking a “core-halo” structure and spreading its density.

Physically, this result can be understood as follows. Suppose that we can artificially divide the system into a hot “core” and a cold “halo”. Since heat flows from hot to cold, the core will lose energy to the benefit of the halo. Since both core and halo have negative specific heats, the core heats up (and shrinks) while the halo cools (and spreads). Therefore the heat transfers continue and the system never achieves equilibrium.

Let us try to formalize this reasoning to show mathematically the absence of a global entropy maximum in an unbounded domain. We describe the core and the halo by a distribution function of the form

$$(15) \quad f = \frac{1}{(2\pi T)^{3/2}} \rho e^{-\frac{v^2}{2T}},$$

where the density  $\rho$  is assumed to be uniform in each subdomain. We denote by  $\rho_c$ ,  $M_c$ ,  $T_c$ ,  $R_c$  and  $\rho_h$ ,  $M_h$ ,  $T_h$ ,  $R_h$  the density, temperature, mass and radius of the core and the halo respectively. With the distribution function (15), we easily find that the kinetic energy and the entropy can be written as

$$(16) \quad K = \frac{3}{2}MT,$$

$$(17) \quad S = \frac{3}{2}M \ln T - M \ln \rho + Cst.$$

It is also easy to compute the potential energy of the core and the halo. Assuming  $R_h \gg R_c$ , we find that

$$(18) \quad W_c = -\frac{3GM_c^2}{5R_c} \quad \text{and} \quad W_h = -\frac{3GM_h M_c}{4R_h} - \frac{3GM_h^2}{5R_h}.$$

We now choose the temperatures  $T_c$  and  $T_h$  so as to satisfy the Virial theorem (12) in each subsystem. The energies of the core and the halo therefore read

$$(19) \quad E_c = -\frac{3}{2}M_c T_c = -\frac{3GM_c^2}{10R_c},$$

$$(20) \quad E_h = -\frac{3}{2}M_h T_h = -\frac{3GM_h M_c}{8R_h} - \frac{3GM_h^2}{10R_h}.$$

In order to conserve the total energy of the system  $E = E_c + E_h$ , the radii of the core and of the halo must satisfy the relation:

$$(21) \quad E = -\frac{3GM_c^2}{10R_c} - \frac{3GM_h M_c}{8R_h} - \frac{3GM_h^2}{10R_h}.$$

We have therefore constructed a particular family of distribution functions parametrized by  $R_h$  that conserves the total mass and the total energy. We now take the limit  $R_h \rightarrow +\infty$  which amounts to spreading the density to infinity. Since the energy of the halo increases, that of the

core must decrease. It results from Eq. (21) that the core shrinks to a minimum radius  $R_c^{min}$  given by

$$(22) \quad R_c^{min} = -\frac{3GM_c^2}{10E}.$$

Its temperature increases up to the maximum value

$$(23) \quad T_c^{max} = \frac{GM_c}{5R_c^{min}} = -\frac{2E}{3M_c},$$

whereas the temperature of the halo decreases to zero like

$$(24) \quad T_h = \frac{GM_c}{4R_h} + \frac{GM_h}{5R_h} \rightarrow 0.$$

Therefore, the entropy of the core remains bounded whereas the entropy of the halo behaves like

$$(25) \quad S_h \sim -\frac{3}{2}M_h \ln R_h + 3M_h \ln R_h \sim \frac{3}{2}M_h \ln R_h,$$

and diverges to  $+\infty$  when we spread the halo to infinity. As a result, there is no global entropy maximum (at fixed mass and energy) in a unbounded domain.

Note that the previous discussion is only valid for  $E \leq 0$  (which is the most relevant case). For  $E > 0$ , we just need to consider a uniform sphere of mass  $M$  and radius  $R$  [19]. The total energy is

$$(26) \quad E = \frac{3}{2}MT - \frac{3GM^2}{5R}.$$

When  $R \rightarrow +\infty$ , the temperature takes the finite value

$$(27) \quad T_{min} = \frac{2E}{3M}.$$

The entropy behaves like

$$(28) \quad S \sim 3M \ln R,$$

and diverges again when we spread the system to infinity.

## 2.4 The infinite mass problem

**Theorem 2:** There is no local entropy maximum in an unbounded domain. Isothermal spheres have an *infinite mass*.

We shall restrict ourselves to spherically symmetric solutions of Eq. (9) since only spherically symmetric states can correspond to local entropy maxima of non rotating systems [12]. In that case, Eq. (9) can be written

$$(29) \quad \frac{1}{r^2} \frac{d}{dr} \left( r^2 \frac{d\Phi}{dr} \right) = 4\pi G A e^{-\beta\Phi}.$$

This equation has been studied extensively in the context of isothermal gaseous spheres [11]. We can check by direct substitution that the distribution

$$(30) \quad \Phi_s(r) = \frac{1}{\beta} \ln(2\pi G \beta A r^2), \quad \rho_s(r) = \frac{1}{2\pi G \beta r^2},$$

is an exact solution of Eq. (29) known as the *singular isothermal sphere* [1]. Since  $\rho \sim r^{-2}$  at large distances, the total mass of the system  $M = \int_0^{+\infty} \rho 4\pi r^2 dr$  is infinite! More generally, we can show that any solution of the mean-field equation (29) behaves like the singular sphere as  $r \rightarrow +\infty$  and has therefore an infinite mass. To show this, let us make the change of variables

$$(31) \quad \Phi = \frac{2}{\beta} \ln r + z, \quad t = \ln r.$$

In terms of these variables, Eq. (29) becomes

$$(32) \quad \frac{d^2 z}{dt^2} + \frac{dz}{dt} + \frac{2}{\beta} = 4\pi G A e^{-\beta z}.$$

Put in the form

$$(33) \quad \frac{d^2 z}{dt^2} + \frac{dz}{dt} = -\frac{d}{dz} \left( \frac{4\pi G A}{\beta} e^{-\beta z} + \frac{2}{\beta} z \right),$$

it corresponds to the damped motion of a particle in a potential  $V(z) = 4\pi G A / \beta e^{-\beta z} + 2z / \beta$  where  $z$  plays the role of position and  $t$  the role of time. The potential has a minimum at  $z_0 = \frac{1}{\beta} \ln(2\pi G \beta A)$ . For large times the motion damps out and the particle comes to rest at the minimum, i.e.  $z \rightarrow z_0$  as  $t \rightarrow +\infty$ . Returning to the original variables, we deduce that for  $r \rightarrow +\infty$

$$(34) \quad \Phi \rightarrow \Phi_s = \frac{1}{\beta} \ln(2\pi G \beta A r^2), \quad \rho \rightarrow \rho_s(r) = \frac{1}{2\pi G \beta r^2},$$

which proves the result.

Physically, the infinite mass problem disappears if we take into account physical processes that are relevant for the system under consideration. Indeed, a system never extends to infinity so the conditions for which statistical mechanics is applicable (regarding for example the ergodic hypothesis) are valid only in a finite region of space. For example, a globular cluster is not isolated but subject to the tides of a neighboring object (e.g., a spiral galaxy). Sufficiently energetic stars (with  $\epsilon > \epsilon_m$ , say, where  $\epsilon_m$  is the escape energy) have elongated orbits and are removed by the tidal field of the object. Therefore the distribution function (7) must be modified near the escape energy. The most famous truncated model is the Michie-King model

$$(35) \quad f = \begin{cases} A'(e^{-\beta\epsilon} - e^{-\beta\epsilon_m}) & \epsilon \leq \epsilon_m, \\ 0 & \epsilon \geq \epsilon_m. \end{cases}$$

This model can be deduced from a Fokker-Planck equation [20, 21] and gives very good fits with the actual distribution function of globular clusters (for moderate density contrasts for which the gravothermal catastrophe does not occur) [1]. For  $\epsilon \ll \epsilon_m$ , the distribution function is almost isothermal and for  $\epsilon > \epsilon_m$ ,  $f = 0$  since stars have escaped. With this cut-off, the star density drops to zero at a finite radius  $r_m$  identified as the tidal radius. Hence, the total mass of the system is finite. Another, more convenient, procedure to solve the infinite mass problem is to confine artificially the system within a box against which the stars bounce elastically. This

model is less realistic but the presence of a wall at radius  $R$  should not dramatically affect the structure of the system at radii  $r \ll R$ . Physically, the radius  $R$  represents the typical size over which statistical mechanics is applicable. The box model was introduced by Antonov [12] and was further explored by Lynden-Bell & Wood [13], Katz [22], Padmanabhan [9], de Vega & Sanchez [23] and Chavanis [18] among others. It is found that even when confined to a box, self-gravitating systems exhibit a peculiar behavior.

## 2.5 Absence of global entropy maximum in a box

**Theorem 3:** There is *no global* entropy maximum in a box. A self-gravitating system can always increase entropy by taking a “core-halo” structure and making its core denser and denser and hotter and hotter.

To understand physically this result, let us again divide the system into a “core” and a “halo”. The core is primarily confined by self-gravity and has a negative specific heat. On the other hand, the halo is held by the box and has a positive specific heat like a usual gas. If the core is momentarily hotter than the halo, heat flows from core to halo and the temperature of both core and halo increases. If  $C_h < |C_c|$ , the temperature of the halo increases more rapidly than the temperature of the core and the heat transfers are shut-off. By contrast, if  $C_h > |C_c|$ , the halo cannot heat up as fast as the core and the temperature difference remains. In that case the system does not reach an equilibrium state.

The absence of global entropy maximum for finite isothermal spheres is well-known [12, 13, 19] but we wish to give a more physical proof of this result based on the previous qualitative discussion. We shall construct a family of distribution functions of the form (15) which conserves mass and energy and for which entropy indefinitely increases as the core shrinks. Since the core has a negative specific heat, we choose its temperature so as to satisfy the Virial relation:

$$(36) \quad E_c = -\frac{3}{2}M_cT_c = -\frac{3GM_c^2}{10R_c}.$$

On the other hand, the energy of the halo can be written

$$(37) \quad E_h = \frac{3}{2}M_hT_h - \frac{3GM_hM_c}{R} - \frac{3GM_h^2}{R},$$

where  $R$  is the box radius. According to Eqs. (36)-(37), we have  $C_c = -\frac{3}{2}M_c < 0$  and  $C_h = \frac{3}{2}M_h > 0$  in agreement with our qualitative discussion. We shall assume that  $M_h > M_c$  to be in the unstable situation ( $C_h > |C_c|$ ). In order to conserve the total energy, the temperature of the halo must be related to the core radius by

$$(38) \quad E = -\frac{3GM_c^2}{10R_c} + \frac{3}{2}M_hT_h - \frac{3GM_hM_c}{R} - \frac{3GM_h^2}{R}.$$

We now take the limit  $R_c \rightarrow 0$  which amounts to shrinking the core. Since the energy of the core goes to  $-\infty$ , the temperature of the halo must increase to  $+\infty$  in order to conserve the total energy. According to Eq. (38) we have:

$$(39) \quad T_h = \frac{GM_c^2}{5M_hR_c} \rightarrow +\infty,$$

while the temperature of the core diverges like

$$(40) \quad T_c = \frac{GM_c}{5R_c} \rightarrow +\infty.$$

Note that  $T_c > T_h$  (if  $M_c < M_h$ ), which is consistent with the direction of heat transfers in an unstable situation. The entropy of the core behaves like

$$(41) \quad S_c \sim -\frac{3}{2}M_c \ln R_c + 3M_c \ln R_c \sim \frac{3}{2}M_c \ln R_c,$$

and the entropy of the halo like

$$(42) \quad S_h \sim -\frac{3}{2}M_h \ln R_c.$$

For the total entropy we have

$$(43) \quad S \sim -\frac{3}{2}(M_h - M_c) \ln R_c.$$

If  $M_h > M_c$ , we find that the entropy goes to  $+\infty$  when  $R_c \rightarrow 0$ , i.e. when we shrink the core. These simple arguments show the *natural* tendency (in a thermodynamical sense) of a stellar system to develop a dense and hot “core” surrounded by a low-density “halo” ( $\rho_h \ll \rho_c$ ). In this sense, no equilibrium state can exist for self-gravitating systems, even in theory ! It is possible, however, that the system settles down on a *local* entropy maximum (metastable state). This is the problem discussed in the next section.

## 2.6 Antonov instability and the gravothermal catastrophe

**Theorem 4:** When a self-gravitating system is confined within a box, *local* entropy maxima exist only for  $\Lambda \equiv -\frac{ER}{GM^2} < \Lambda_c$  with  $\Lambda_c = 0.3345\dots$ ; they have a density contrast  $\mathcal{R} = \rho(0)/\rho(R) \lesssim 709$ . Critical points of entropy with density contrast  $\mathcal{R} \gtrsim 709$  are unstable saddle points. For  $\Lambda > \Lambda_c$ , there are no critical points of entropy.

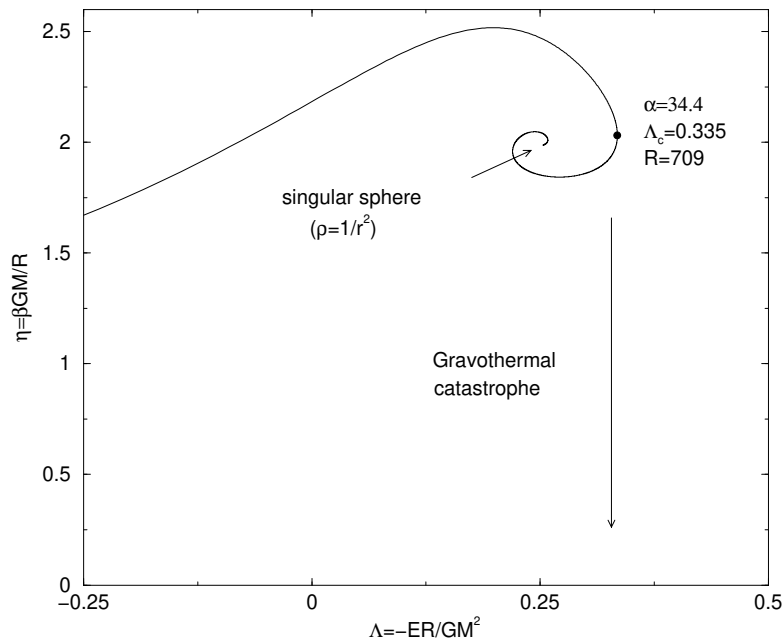


Figure 1: Stability diagram for isothermal spheres in the microcanonical ensemble (fixed  $E$ ).

The equilibrium diagram is represented on Fig. 1, where we have plotted the normalized inverse temperature  $\eta = \beta GM/R$  as a function of  $\Lambda = -ER/GM^2$  [1]. Increasing  $\Lambda$  amounts

to decreasing the energy  $E$  at fixed volume or to increasing the box radius  $R$  at fixed energy. Each point on the curve corresponds to a critical point of entropy, i.e. a solution of Eq. (29). The curve can be parametrized by the density contrast  $\mathcal{R} = \rho(0)/\rho(R)$  which increases monotonically from 1 to  $+\infty$  as we spiral inward. It is possible to prove the following results [9]:

(i) For  $\Lambda < \Lambda_c$  the solutions on the upper branch are local entropy maxima. They have a smooth density profile and a relatively low density contrast  $\mathcal{R} \lesssim 709$ .

(ii) For  $\Lambda > \Lambda_c$ , there are no critical points of entropy, i.e. no statistical equilibrium [12] ! In that case, the system is expected to collapse and overheat. This is the so-called “gravothermal catastrophe” or “Antonov instability” [13]. As discussed by Lynden-Bell & Wood [13], this instability is probably related to the negative specific heats of self-gravitating systems: by loosing heat, the core grows hotter and evolves away from equilibrium (see section 2.5). The “gravothermal catastrophe” has been confirmed by sophisticated numerical simulations of globular clusters that introduce a precise description of heat transfers between the “core” and the “halo” using moment equations [24], orbit averaged Fokker-Planck equation [25] or fluid equations for a thermally conducting gas [26]. In these studies, the collapse proceeds self-similarly and the central density becomes infinite in a finite time. This singularity has been known as “core collapse” and many globular clusters have probably experienced core collapse. This is certainly the most exciting theoretical aspect of the collisional evolution of stellar systems. In practice, the formation of hard binaries can release sufficient energy to stop the collapse and even drive a re-expansion of the system [14]. Then, a series of gravothermal oscillations should follow [15]. It has to be noted that, although the central density tends to infinity, the mass contained in the core tends to zero so, in this sense, the gravothermal catastrophe is a rather unspectacular process [1]. However, the gravothermal catastrophe can also be at work in dense clusters of compact stars (neutron stars or stellar mass black holes) embedded in evolved galactic nuclei and it can presumably initiate the formation of super-massive black holes via the collapse of such clusters. Indeed, when the central red-shift (related to the density contrast) exceeds a critical value  $z_c \sim 0.5$ , a dynamical instability of general-relativistic origin sets in and the star cluster undergoes a catastrophic collapse to a black hole on a dynamical time scale. It can be shown that this process leads naturally to the birth of super-massive black holes of the right size to explain quasars and AGNs [27].

(iii) For  $\Lambda < \Lambda_c$  and  $\mathcal{R} \gtrsim 709$ , there are critical points of entropy but they are saddle points. Therefore, a second order perturbation can drive the system along the valley of the saddle point. The unstable curve spirals to the point  $(1/4, 2)$  which corresponds to the singular sphere ( $\mathcal{R} = \infty$ ).

The stability of the solutions can be deduced from the topology of the  $\beta - E$  curve by using the method of Katz [22] who has extended Poincaré’s theory of linear series of equilibrium. The parameter conjugate to the entropy with respect to energy is the inverse temperature  $\beta = (\partial S / \partial E)_{M,R}$ . Then, if we plot  $\beta$  as a function of  $-E$  (at fixed mass and radius) as in Fig. 1, we have the following results: (i) a change of stability can occur only at a limit point where  $E$  is an extremum ( $d\beta/dE$  infinite). (ii) a mode of stability is lost when the curve rotates clockwise and gained otherwise. Now, we know that for  $E$  sufficiently large the solutions are stable because, in this limit, self-gravity is negligible and the system behaves like an ordinary gas. From point (i) we conclude that the whole upper branch is stable. As the curve spirals inward for  $\mathcal{R} > 709$ , more and more modes of stability are lost. In this respect, the singular sphere, at the end of the spiral, is the most unstable solution. These general results are not dependent on the box model. Lynden-Bell and Wood [13] and Katz [28] have investigated various truncated models, including the Michie-King model (35), and found that the gravothermal catastrophe occurs in each model.

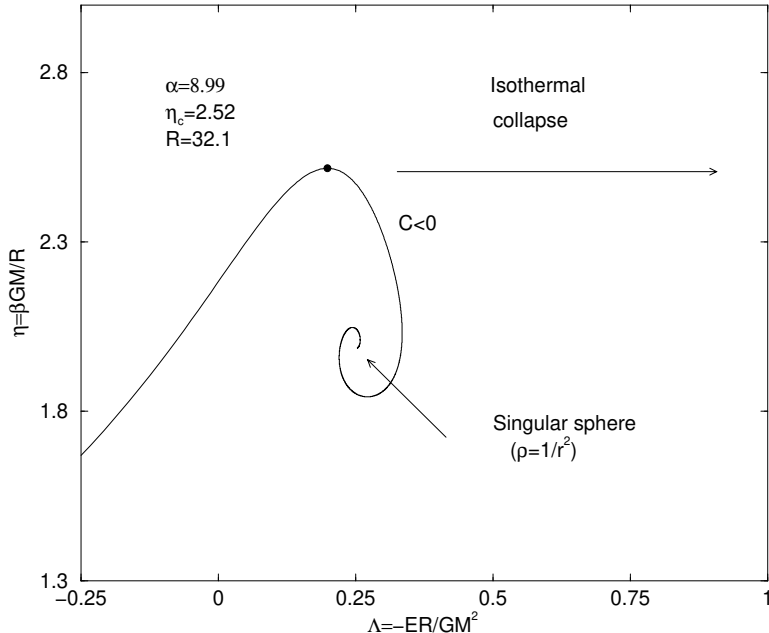


Figure 2: Stability diagram for isothermal spheres in the canonical ensemble (fixed  $T$ ).

## 2.7 Self-gravitating systems at fixed temperature

So far, we have considered the microcanonical ensemble corresponding to an isolated system with constant energy. We now turn to the canonical ensemble where the system is at a fixed temperature  $T$ . The relevant thermodynamical function is now the free energy

$$(44) \quad J = S - \beta E,$$

which must be maximum at fixed  $T$  and  $M$ , to get a stable equilibrium state. It is possible to prove the following results [13, 22, 18]:

**Theorem 5:** When a self-gravitating system is confined within a box and kept at a fixed temperature  $T$ , *local* maxima of free energy exist only for  $\eta \equiv \frac{\beta GM}{R} < \eta_c$  with  $\eta_c = 2.517\dots$ ; they have a density contrast  $\mathcal{R} = \rho(0)/\rho(R) \lesssim 32.1$ . Critical points of free energy with density contrast  $\mathcal{R} \gtrsim 32.1$  are unstable saddle points. For  $\eta > \eta_c$ , there are no critical points of free energy.

The critical points of  $J$  with the previous constraints are still given by Eq. (7) and the equilibrium diagram giving  $-E$  as a function of  $\beta$  can be deduced from Fig. 2 by a rotation of  $\pi/2$ . By inspection of this figure, we see that there are no critical points of the free energy for  $\eta > \eta_c$ . We expect therefore that sufficiently cold systems will collapse. This “isothermal collapse” is the counterpart of the “gravothermal catastrophe” in the microcanonical ensemble. The stability of the critical points can be deduced from the method of Katz [22]. Using Eq. (6), we have

$$(45) \quad \delta J = -E\delta\beta + \alpha\delta M,$$

so that the parameter conjugate to the free energy with respect to the inverse temperature  $\beta$  is  $-E = (\frac{\partial J}{\partial \beta})_{M,R}$ . Considering Fig. 2 again, we find that the change of stability occurs at the maximum inverse temperature  $\eta = \eta_c$ . This corresponds to a density contrast of  $\sim 32.1$ . Therefore, critical points with density contrast  $\mathcal{R} \gtrsim 32.1$  are unstable saddle points. In fact,

the reason for the instability is clear if we notice that, for  $32.1 \lesssim \mathcal{R} \lesssim 709$ , the specific heat  $C = dE/dT$  is negative. This is not possible in the canonical ensemble where, quite generally, the specific heat *must* be positive [9]. By contrast, thermally isolated systems can have negative specific heats: in the microcanonical ensemble, the solutions with  $32.1 \lesssim \mathcal{R} \lesssim 709$  are stable (see section 2.6). This clearly demonstrates that the statistical ensembles do not coincide for self-gravitating systems: the region of negative specific heats in the microcanonical ensemble is replaced by a phase transition in the canonical ensemble [9].

## 2.8 Self-gravitating fermions and the violent relaxation of collisionless stellar systems

We now briefly discuss the equilibrium states of self-gravitating systems described by the Fermi-Dirac entropy

$$(46) \quad S = - \int \{f \ln f + (\eta_0 - f) \ln(\eta_0 - f)\} d^3\mathbf{r} d^3\mathbf{v},$$

instead of the Boltzmann entropy (5). The entropy (46) represents the natural form of entropy for quantum particles (fermions) such as degenerate electrons in White Dwarf stars [11] or massive neutrinos in Dark Matter models [29]. In that case  $\eta_0 = g/h^3$  (where  $h$  is the Planck constant and  $g = 2s+1$  is the spin multiplicity of quantum states) corresponds to the maximum allowable value of the distribution function imposed by the Pauli exclusion principle. The entropy (46) has also been proposed for collisionless stellar systems (like elliptical galaxies) undergoing a “violent relaxation” towards a virialized state [2]. In this context,  $\eta_0$  represents the maximal value of the initial distribution function and the actual distribution function (coarse-grained) must always satisfy  $\bar{f} \leq \eta_0$  by virtue of the Liouville theorem. This is the origin of the effective exclusion principle in Lynden-Bell’s theory [2].

Introducing Lagrange multipliers like in Eq. (6), we find that the critical points of entropy at fixed mass and energy correspond to the Fermi-Dirac distribution function

$$(47) \quad f = \frac{\eta_0}{1 + \lambda e^{\beta(\frac{v^2}{2} + \Phi)}},$$

where  $\lambda$  is a strictly positive constant insuring that  $f \leq \eta_0$ . In the fully degenerate limit  $f \simeq \eta_0$ , this distribution function has been extensively studied in the context of White Dwarf stars in which gravity is balanced by the pressure of a degenerate electron gas [11]. In the non degenerate limit  $f \ll \eta_0$ , the Fermi-Dirac distribution reduces to the Maxwell-Boltzmann distribution

$$(48) \quad f \simeq \frac{\eta_0}{\lambda} e^{-\beta(\frac{v^2}{2} + \Phi)},$$

so we expect to recover the results of sections 2.1-2.7 at low densities.

Kinetic equations have been proposed to describe the relaxation of a self-gravitating system towards the Fermi-Dirac distribution [30, 31, 4, 6, 7]. If we allow for high energy particles to escape the system when they reach an energy  $\epsilon \geq \epsilon_m$ , an extension of the Michie-King model (35) taking into account the degeneracy can be deduced from these equations as shown by Chavanis [6]. For  $\epsilon < \epsilon_m$ , one has:

$$(49) \quad f = \eta_0 \frac{e^{-\beta\epsilon} - e^{-\beta\epsilon_m}}{\lambda + e^{-\beta\epsilon}},$$

while  $f = 0$  for  $\epsilon > \epsilon_m$ . When  $\lambda \rightarrow +\infty$ , we recover the Michie-King model (35) and when  $\epsilon_m \rightarrow +\infty$  we recover the Fermi-Dirac distribution (47). This distribution function could describe galactic halos limited in extension as a consequence of tidal interactions with other systems [29]. In the artificial situation in which the system is enclosed within a spherical box, it is possible to prove the following results [5, 19]:

**Theorem 6:** For self-gravitating fermions (or collisionless stellar systems) confined within a box, there exists a global entropy maximum for all accessible values of energy. If the temperature is fixed instead of the energy, there exists a global maximum of free energy for each temperature. For low energies or low temperatures, this global maximum has a “core-halo” structure with a degenerate core and a non degenerate halo.

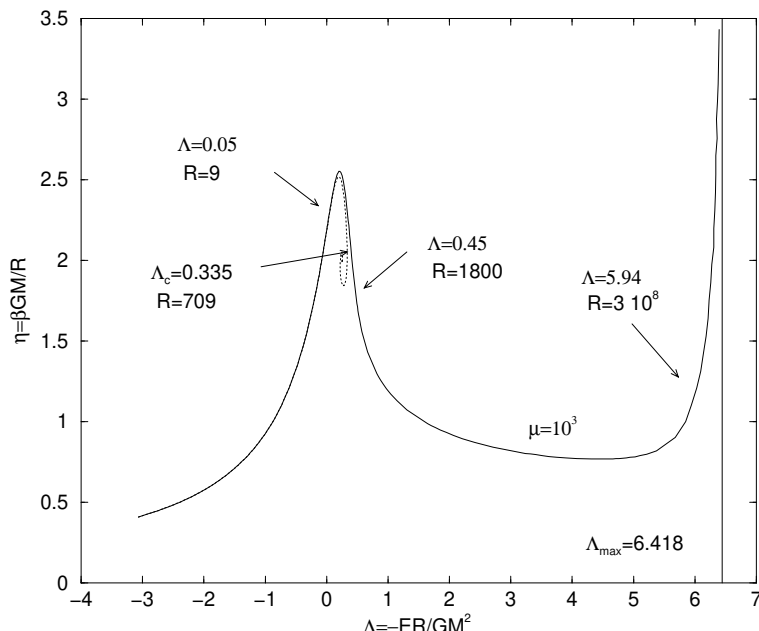


Figure 3: Equilibrium diagram for Fermi-Dirac spheres ( $\mu = 10^3$ ).

Therefore, degeneracy has a stabilizing role and is able to stop the “gravothermal catastrophe” or the “isothermal collapse”. The computation of Fermi-Dirac spheres has been performed by Chavanis & Sommeria [5]. The extension of the classical diagram of Fig. 1 is reported on Figs. 3 and 4. We see that the inclusion of degeneracy has the effect of unwinding the spiral. When the degeneracy parameter  $\mu = \eta_0/\langle f \rangle \equiv \eta_0 \sqrt{512\pi^4 G^3 M R^3}$  is small (Fig. 3) there is only one critical point of entropy for each value of  $\Lambda$  and it is a global entropy maximum. For small values of  $\Lambda$  (high energies) the solutions almost coincide with the classical (non degenerate) isothermal spheres. When  $\Lambda$  is increased (low energies) the solutions become partially degenerate and it is now possible to overcome the critical value  $\Lambda_c$  (or the density contrast  $\mathcal{R} \simeq 709$ ) of Antonov. When  $\Lambda = \Lambda_{max}$ , the core is completely degenerate and contains all the mass and energy. In that case, the system has the same structure as a cold White Dwarf star. In this somewhat singular limit, the system is self-confined and the box is not needed [11]. When the degeneracy parameter  $\mu$  is large (see Fig 4), there are several critical points of entropy for each single value of the energy in the range  $\Lambda_* < \Lambda < \Lambda_c$ . The solutions on the upper branch (points A) are non degenerate and have a smooth density profile while the solution on the lower branch (points C) have a “core-halo” structure with a degenerate nucleus. According to the theorem of Katz, they are both entropy maxima while the intermediate solutions, points B, are

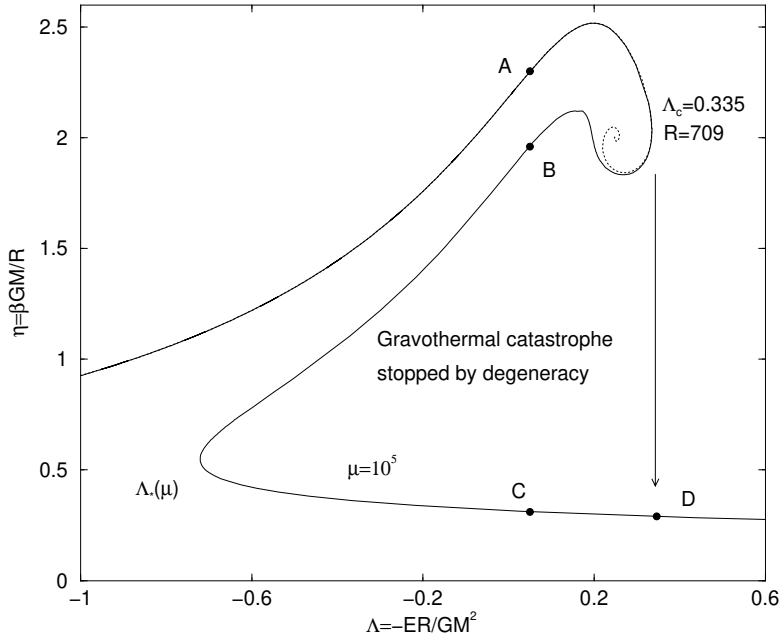


Figure 4: Equilibrium diagram for Fermi-Dirac spheres ( $\mu = 10^5$ ).

unstable saddle points. For small values of  $\Lambda$ , the non degenerate solutions (upper branch) are global entropy maxima. They become local entropy maxima (metastable states) at a certain  $\Lambda_t \geq \Lambda_*$  determined by a Maxwell construction (of course  $\Lambda_t \rightarrow -\infty$  as  $\mu \rightarrow +\infty$ ). At that  $\Lambda_t$ , the degenerate solutions (lower branch) that were only local entropy maxima suddenly become global entropy maxima. We expect therefore a phase transition to occur between the “gaseous” phase (upper branch) and the “condensed” phase (lower branch) at  $\Lambda_t$ . We may suspect [5], however, that the entropic barrier is so hard to cross that, in general, the system still prefers the metastable solutions on the upper branch for  $\Lambda > \Lambda_t$  (in other words, the “bassin of attraction” of the non degenerate solutions is wider). Therefore, the true phase transition will occur at  $\Lambda_c$  at which the upper branch completely disappears: at that point, the gravothermal catastrophe occurs, but, for systems described by the Fermi-Dirac statistics, the core ultimately ceases to shrink when it becomes degenerate. In that case, the system falls on to the global entropy maximum which is the true equilibrium state for these systems. This global entropy maximum has a “core-halo” structure, with a degenerate core and a non degenerate halo. Similar phase transitions appear in the canonical ensemble where the temperature is fixed instead of the energy. A more general discussion on the equilibrium states of self-gravitating fermions can be found in Ref. [5]. Considering a classical gas with a short distance cut-off  $a$  essentially leads to the same results [9, 32] ( $a/R$  plays the role of  $1/\mu$ ).

For astrophysical purposes, it is still a matter of debate to decide whether collisionless stellar systems like elliptical galaxies are degenerate (in the sense of Lynden-Bell) or not. Since degeneracy can stabilize the system without changing its overall structure at large radii, it has been suggested that degeneracy could play a role in galactic nuclei [2, 5]. The recent numerical simulations of Leeuwin & Athanassoula [33] and the theoretical model of Stiavelli [34] are consistent with this idea especially if the nucleus of elliptical galaxies contains a massive black hole. Indeed, the effect of degeneracy on the distribution of stars produced by the black hole can explain the cusps observed at the center of galaxies [34]. This form of degeneracy is also relevant for massive neutrinos in Dark Matter models where it competes with quantum degeneracy [35]. In fact, the Fermi-Dirac distribution for collisionless Dark Matter (e.g., massive neutrinos) might be justified more by the process of “violent relaxation” [2] than by quantum

mechanics [29] (see Ref. [7] for more details).

It should be finally emphasized that the theory of violent relaxation developed by Lynden-Bell is conditioned by an hypothesis of ergodicity which may not be completely fulfilled. In practice, the relaxation is *incomplete* and the final distribution function may significantly differ from the Fermi-Dirac distribution (47). One of the reasons is that fluctuations in the gravitational potential are efficient only in a limited region of space (the main body of the galaxy) and persist only for a finite amount of time (they decay as the system approaches equilibrium) [4]. Hjorth & Madsen [36] have derived a truncated model for elliptical galaxies by assuming that violent relaxation proceeds to completion in a finite spatial region of radius  $R$  and that, subsequently, high energy stars leave that region and move in orbit beyond  $R$ , thereby changing this part of the distribution to a power-law with index  $\sim 5/2$ . Their model provides a very good fit with the surface-brightness distribution of elliptical galaxies. An alternative truncated model proposed by Stiavelli & Bertin [37] and incorporating an angular momentum cut-off in the distribution function gives an equally good fit. These models assume that the galaxy is isolated. If, on the other hand, the galaxy is gravitationally affected by other systems, the time variations of the gravitational potential induced by external forces can make the galaxy relax towards the truncated distribution function (49). For our present purpose, we shall assume that the system is confined within a spherical box and that violent relaxation proceeds to completion in this idealized system.

### 3 A simple dynamical model for the violent relaxation of stellar systems towards statistical equilibrium

#### 3.1 The Smoluchowki-Poisson system

In previous works [3, 4, 6, 7] (see also Ref. [2]), we have proposed to describe the violent relaxation of stellar systems towards thermodynamical equilibrium by a phenomenological Fokker-Planck equation

$$(50) \quad \frac{\partial \bar{f}}{\partial t} + \mathbf{v} \frac{\partial \bar{f}}{\partial \mathbf{r}} + \mathbf{F} \frac{\partial \bar{f}}{\partial \mathbf{v}} = \frac{\partial}{\partial \mathbf{v}} \left\{ D \left( \frac{\partial \bar{f}}{\partial \mathbf{v}} + \beta \bar{f} \mathbf{v} \right) \right\},$$

coupled with the Poisson equation (4). This equation involves a diffusion in velocity space, arising from the rapid fluctuations of the gravitational potential, compensated by a dynamical friction  $-\xi \mathbf{v}$ . The friction is probably related to a kind of collisionless Landau damping and it ensures the convergence towards a maximum entropy state, as predicted by Lynden-Bell [2]. The friction coefficient is given by an Einstein formula  $\xi = D\beta$  which is a consequence of the “fluctuation-dissipation” theorem. Of course, Eq. (50) is valid for the coarse-grained distribution function  $\bar{f}$  since the fine-grained distribution function  $f$  is conserved by the Vlasov equation (in the collisionless regime) and does not undergo a diffusion process. Rigorously speaking, the friction term is of the form  $-D\beta(\eta_0 - \bar{f})\mathbf{v}$  so as to account for the exclusion principle implied by the Liouville theorem [4]. Although the theory can easily take into account degeneracy effects, we shall restrict ourselves in the following to the non degenerate limit  $\bar{f} \ll \eta_0$  for which the equations are simpler. Therefore, our study will cease to be valid when the system becomes “too” dense. The maximum allowable density (in physical space) depends on the value of the degeneracy parameter  $\mu$  in a non trivial way [5]. If the degeneracy parameter  $\mu$  is sufficiently large, very high densities can be allowed. For example, our model can describe the early stage of the gravitational collapse depicted in Fig. 4 before degeneracy effects come into play.

By analogy with Brownian theory, we expect the distribution function to thermalize after a transient regime of order  $\xi^{-1}$ . Then, the star density (in physical space) will be described by the Smoluchowski equation

$$(51) \quad \frac{\partial \rho}{\partial t} = \nabla \left\{ \frac{1}{\xi} (T \nabla \rho + \rho \nabla \Phi) \right\}.$$

The passage from the Fokker-Planck equation to the Smoluchowski equation is rigorous in a limit of strong friction  $\xi \rightarrow +\infty$  [38, 39, 4, 7], for which the velocity of the particles becomes proportional to the force, i.e.

$$(52) \quad \mathbf{u} = -\frac{1}{\xi} \left( \frac{T}{\rho} \nabla \rho + \nabla \Phi \right),$$

where  $-(T/\rho) \nabla \rho$  is the pressure force and  $-\nabla \Phi$  the gravitational force. In that case, the Smoluchowski equation (51) can be interpreted as a continuity equation with velocity (52). In the present context,  $\xi^{-1}$  is of the order of the dynamical time  $t_D$  so, contrary to the ideal Brownian theory, the Smoluchowski equation is only marginally valid. Our aim here is not to develop an exact kinetic theory of collisionless relaxation (see Refs. [30, 31, 6, 7] for a starting point in the quasilinear approximation) but rather to introduce a simple relaxation equation which is consistent with the first and second principles of thermodynamics and which is easy to handle numerically and analytically. The Smoluchowski equation has been studied extensively in the case of an external potential [39] and it is clearly of great interest to consider the extension of this study when the potential is not fixed but related to the density via a Poisson equation, like in the gravitational case.

### 3.2 The Maximum Entropy Production Principle

The relaxation equation (51) is consistent with a Maximum Entropy Production Principle (M.E.P.P.) [4]. It provides therefore a simple numerical algorithm to calculate maximum entropy states at fixed mass and energy (or temperature) and study dynamically the phase transitions in self-gravitating systems. As indicated previously, we restrict ourselves to the Boltzmann entropy (5), appropriate to the nondegenerate limit, but our procedure can be easily extended to the Fermi-Dirac entropy (46) or any other functional [4]. To construct our algorithm, we proceed in two steps. First, we maximize entropy at fixed mass  $M$ , energy  $E$  and density  $\rho(\mathbf{r}, t)$ . This problem always has a solution, the Maxwellian distribution:

$$(53) \quad \bar{f}(\mathbf{r}, \mathbf{v}, t) = \frac{1}{(2\pi T(t))^{3/2}} \rho(\mathbf{r}, t) e^{-\frac{v^2}{2T(t)}},$$

which is a global maximum for  $S$  subject to the previous constraints [9]. It is now possible to express the energy and the entropy in terms of the star density  $\rho(\mathbf{r}, t)$  and the temperature  $T(t)$  in the form

$$(54) \quad E = \frac{3}{2} M T + \frac{1}{2} \int \rho \Phi d^3 \mathbf{r},$$

$$(55) \quad S = \frac{3}{2} M + \frac{3}{2} M \ln(2\pi T) - \int \rho \ln \rho d^3 \mathbf{r}.$$

We then determine the evolution of the density  $\rho(\mathbf{r}, t)$  which maximizes the rate of entropy production  $\dot{S}$  at fixed mass and energy. This Maximum Entropy Production Principle leads to an equation of the form [4, 3, 7]:

$$(56) \quad \frac{\partial \rho}{\partial t} = \nabla \left[ \frac{1}{\xi} (T(t) \nabla \rho + \rho \nabla \Phi) \right],$$

in which the temperature  $T(t)$  is determined by the energy constraint (54) and the gravitational potential  $\Phi$  is related to the star density  $\rho$  by the Poisson equation (4). The parameter  $\xi$  is undetermined by the MEPP but it is related to an inverse characteristic time of order  $t_D$  (the dynamical time) which can be determined with a quasilinear theory [6]. For the purpose of calculating maximum entropy states (or exhibiting phase transitions), it is sufficient to assume that  $\xi$  is constant and we shall make this choice in the following (it might also be relevant to consider the case  $\xi \sim t_D^{-1} \sim \sqrt{G\rho}$ ). The Fokker-Planck equation (50) can also be obtained from the MEPP by relaxing the assumption (53) that  $f$  is isothermal (see Ref. [4] for a precise account). Clearly, the Fokker-Planck-Poisson system is more appropriate than the Smoluchowski-Poisson system but it is also more difficult to solve numerically as it lives in a six-dimensional phase space.

Taking the time derivative of Eq. (55) and using Eqs. (54)-(56), we find that

$$(57) \quad \dot{S} = \int \frac{1}{T\rho\xi} (T \nabla \rho + \rho \nabla \Phi)^2 d^3 \mathbf{r}.$$

Therefore, the entropy increases monotonically provided that  $\xi > 0$ . At equilibrium (if it exists !), the term in bracket cancels out and we recover the Boltzmann distribution (8). If we fix the temperature instead of the energy, we find in the same manner that the free energy (44) monotonically increases. Eqs. (56)(54)(4) therefore provide a simple numerical algorithm to compute maximum entropy states and check Antonov instability when such maxima do not exist. One interest of our study is to satisfy the strict conditions of statistical mechanics, i.e. keep  $E, M, R$  (or  $T, M, R$ ) constant, and be able to vary these parameters easily from one numerical experiment to the other. Therefore, we can cover the whole bifurcation diagram in parameter space and check, by an independent method, the stability limits of Katz [22] and Padmanabhan [17].

To close our system of equations, we must specify the boundary conditions. In the following, we shall assume that the confining box is spherical and restrict ourselves to spherically symmetric solutions. In that case, the boundary conditions are:

$$(58) \quad \frac{\partial \Phi}{\partial r}(0) = 0, \quad \Phi(R) = -\frac{GM}{R},$$

$$(59) \quad T \frac{\partial \rho}{\partial r} + \rho \frac{\partial \Phi}{\partial r} = 0, \quad \text{at } r = R.$$

The first condition expresses the fact that the gravitational force at the center of a spherically symmetric system is zero. The second condition defines the gauge constant in the gravitational potential. Finally, the last condition insures that the total mass is conserved. Multiplying the Poisson equation

$$(60) \quad \frac{1}{r^2} \frac{\partial}{\partial r} \left( r^2 \frac{\partial \Phi}{\partial r} \right) = 4\pi G\rho,$$

by  $r^2$  and integrating from 0 to  $r$ , we find that

$$(61) \quad \frac{\partial \Phi}{\partial r}(r) = \frac{GM(r)}{r^2} = \frac{G}{r^2} \int_0^r \rho(r') 4\pi r'^2 dr',$$

where  $M(r)$  is the mass contained in the sphere of radius  $r$ . This result is well-known in potential theory: the gravitational force  $\mathbf{F} = -md\Phi/dre_r$  created by a spherically symmetric distribution of matter in  $r$  depends only on the matter inside the sphere of radius  $r$ , and is equal to the force due to a point of mass  $M(r)$  located at the center of the system (Newton-Gauss theorem). Applying this result at  $r = R$ , the boundary condition (59) can be rewritten

$$(62) \quad T \frac{\partial \rho}{\partial r} + \rho \frac{GM}{R^2} = 0, \quad \text{at } r = R.$$

The relaxation equation (56) can also be obtained from the linear thermodynamics of Onsager: indeed, the diffusion current that appears in Eq. (56) is assumed to be proportional to the difference between the pressure force  $T\nabla\rho$  and the gravitational force  $-\rho\nabla\Phi$ . At equilibrium, the two terms balance each other and the Boltzmann distribution establishes itself. The relaxation equation (56) provides therefore a simplified model of “violent relaxation” by which a system out of mechanical equilibrium tries to reach a maximum entropy state on a few dynamical times  $t_D$ . In that case, thermal processes are not the driving mechanism (the evolution is primarily due to the departure from mechanical equilibrium) and it is reasonable to assume that  $T(t)$  is uniform in a first approximation. The opposite assumptions are made in the case of collisional systems, such as globular clusters: in the studies of Larson [24], Cohn [25] and Lynden-Bell & Eggleton [26], the systems are assumed to be in mechanical equilibrium and the evolution (that takes place on the relaxation time scale  $t_R \gg t_D$ ) is due to the thermal gradients between the core and the halo (see section 2.5).

### 3.3 Linear stability analysis

We now perform a linear stability analysis of our relaxation equation. Let  $\rho$ ,  $T$  and  $\Phi$  refer to a stationary solution of Eq. (56) and consider a small perturbation  $\delta\rho$ ,  $\delta T$  and  $\delta\Phi$  around this solution that does not change energy and mass. Since a stationary solution of the relaxation equation is a critical point of entropy we must assume  $\Lambda \leq \Lambda_c$  for a solution to exist. Writing  $\delta\rho \sim e^{\lambda t}$  and expanding Eq. (56) to first order, we find that

$$(63) \quad \lambda\delta\rho = \frac{1}{r^2} \frac{d}{dr} \left[ \frac{r^2}{\xi} \left( \delta T \frac{d\rho}{dr} + T \frac{d\delta\rho}{dr} + \delta\rho \frac{d\Phi}{dr} + \rho \frac{d\delta\Phi}{dr} \right) \right].$$

It is convenient to introduce the notation

$$(64) \quad \delta\rho = \frac{1}{4\pi r^2} \frac{dq}{dr}.$$

Physically,  $q$  represents the mass perturbation  $q(r) \equiv \delta M(r) = \int_0^r 4\pi r'^2 \delta\rho(r') dr'$  within the sphere of radius  $r$ . It satisfies therefore the boundary conditions  $q(0) = q(R) = 0$ . Substituting Eq. (64) in Eq. (63) and integrating, we obtain

$$(65) \quad \frac{\lambda\xi}{r^2} q = 4\pi \delta T \frac{d\rho}{dr} + T \frac{d}{dr} \left( \frac{1}{r^2} \frac{dq}{dr} \right) + \frac{1}{r^2} \frac{dq}{dr} \frac{d\Phi}{dr} + 4\pi \rho \frac{d\delta\Phi}{dr},$$

where we have used  $q(0) = 0$  to eliminate the constant of integration. Using the stationary condition

$$(66) \quad T \frac{d\rho}{dr} + \rho \frac{d\Phi}{dr} = 0,$$

we can rewrite our equation (65) as

$$(67) \quad \frac{\lambda\xi}{4\pi\rho Tr^2}q = -\frac{\delta T}{T^2} \frac{d\Phi}{dr} + \frac{1}{4\pi\rho} \frac{d}{dr} \left( \frac{1}{r^2} \frac{dq}{dr} \right) - \frac{1}{4\pi\rho^2} \frac{1}{r^2} \frac{dq}{dr} \frac{d\rho}{dr} + \frac{1}{T} \frac{d\delta\Phi}{dr},$$

or, alternatively,

$$(68) \quad \frac{d}{dr} \left( \frac{1}{4\pi\rho r^2} \frac{dq}{dr} \right) + \frac{1}{T} \frac{d\delta\Phi}{dr} - \frac{\lambda\xi}{4\pi\rho Tr^2}q - \frac{\delta T}{T^2} \frac{d\Phi}{dr} = 0.$$

Taking the variation of Eq. (61), we obtain

$$(69) \quad \frac{d\delta\Phi}{dr} = \frac{Gq}{r^2}.$$

Therefore,

$$(70) \quad \frac{d}{dr} \left( \frac{1}{4\pi\rho r^2} \frac{dq}{dr} \right) + \frac{Gq}{Tr^2} - \frac{\lambda\xi}{4\pi\rho Tr^2}q - \frac{\delta T}{T^2} \frac{d\Phi}{dr} = 0.$$

From the energy constraint (54) we find that

$$(71) \quad \delta T = -\frac{2}{3M} \int_0^R \delta\rho \Phi 4\pi r^2 dr.$$

Inserting the relation (64) in Eq. (71) and integrating by parts, we obtain

$$(72) \quad \delta T = -\frac{2}{3M} \int_0^R \frac{dq}{dr} \Phi dr = \frac{2}{3M} \int_0^R q \frac{d\Phi}{dr} dr.$$

Hence, our linear stability analysis leads to the eigenvalue equation

$$(73) \quad \frac{d}{dr} \left( \frac{1}{4\pi\rho r^2} \frac{dq}{dr} \right) + \frac{Gq}{Tr^2} - \frac{2V}{3MT^2} \frac{d\Phi}{dr} = \frac{\lambda\xi}{4\pi\rho Tr^2}q,$$

where

$$(74) \quad V = \int_0^R q \frac{d\Phi}{dr} dr,$$

where we recall that  $q(0) = q(R) = 0$ . Eq. (73) is similar to the eigenvalue equation associated with the second order variations of entropy found by Padmanabhan [17]. In particular, they coincide for marginal stability ( $\lambda = 0$ ). More generally, it is proven in Appendix C that a stationary solution of Eq. (56) is linearly stable if and only if it is a local entropy maximum. Our approach therefore provides a dynamical algorithm for analyzing the existence and the stability of isothermal spheres. The zero eigenvalue equation was solved by Padmanabhan [17] by using a very clever trick that avoids computing numerically the equilibrium distribution. It is found that marginal stability occurs at  $\Lambda = \Lambda_c$ , in agreement with Katz [22] approach, and that the perturbation  $\delta\rho/\rho$  that induces instability (technically the eigenfunction associated

with  $\lambda = 0$ ) has a “core-halo” structure. It is also argued qualitatively that the number of oscillations in the profile  $\delta\rho/\rho$  increases as we proceed along the spiral of Fig. 1 up to the singular sphere. Of course, on the upper branch of Fig. 1 the eigenvalues  $\lambda$  are all negative (stability) while more and more eigenvalues become positive (instability) as we spiral inward for  $\mathcal{R} > 709$ .

If we fix the temperature  $T$  instead of the energy  $E$ , the eigenvalue equation becomes (take  $\delta T = 0$  in Eq. (70)):

$$(75) \quad \frac{d}{dr} \left( \frac{1}{4\pi\rho r^2} \frac{dq}{dr} \right) + \frac{Gq}{Tr^2} = \frac{\lambda\xi}{4\pi\rho Tr^2} q.$$

This is similar to the equation found by Chavanis [18] by analyzing the second order variations of the free energy (44). The case of marginal stability ( $\lambda = 0$ ) is obtained for  $\eta = \eta_c$  like in Katz [22] analysis. It should be emphasized that the perturbation  $\delta\rho/\rho$  that induces instability at  $\eta = \eta_c$  in the canonical ensemble has *not* a “core-halo” structure [18].

## 4 Self-similar solutions of the Smoluchowski-Poisson system

### 4.1 Formulation of the general problem

We now try to describe the collapse regime and look for self-similar solutions of our relaxation equation (56). Restricting ourselves to spherically symmetric solutions, this equation becomes

$$(76) \quad \frac{\partial\rho}{\partial t} = \frac{1}{r^2} \frac{\partial}{\partial r} \left\{ \frac{r^2}{\xi} \left( T \frac{\partial\rho}{\partial r} + \rho \frac{\partial\Phi}{\partial r} \right) \right\},$$

where  $\Phi$  is determined by the Poisson equation (4). Using the Gauss theorem (61), we obtain the self-consistent integrodifferential equation:

$$(77) \quad \frac{\partial\rho}{\partial t} = \frac{1}{r^2} \frac{\partial}{\partial r} \left\{ \frac{r^2}{\xi} \left( T \frac{\partial\rho}{\partial r} + \frac{1}{r^2} G\rho \int_0^r \rho(r') 4\pi r'^2 dr' \right) \right\}.$$

We look for self-similar solutions in the form

$$(78) \quad \rho(r, t) = \rho_0(t) f\left(\frac{r}{r_0(t)}\right), \quad r_0 = \left(\frac{T}{G\rho_0}\right)^{1/2},$$

where the density  $\rho_0(t)$  is of the same order as the central density  $\rho(0, t)$  and the radius  $r_0$  is of the same order as the King radius

$$(79) \quad r_K = \left(\frac{9T}{4\pi G\rho(0)}\right)^{1/2},$$

which gives a good estimate of the core radius of a stellar system [1]. Substituting the *ansatz* (78) into equation (77) we find that

$$(80) \quad \frac{d\rho_0}{dt} f(x) - \frac{\rho_0}{r_0} \frac{dr_0}{dt} x f'(x) = \frac{G\rho_0^2}{\xi} \frac{1}{x^2} \frac{d}{dx} \left\{ x^2 \left( f'(x) + \frac{1}{x^2} f(x) \int_0^x f(x') 4\pi x'^2 dx' \right) \right\},$$

where we have set  $x = r/r_0$ . The variables of position and time separate providing that there exists  $\alpha$  such that

$$(81) \quad \rho_0 r_0^\alpha \sim 1.$$

In that case, Eq. (80) reduces to

$$(82) \quad \frac{d\rho_0}{dt} \left( f(x) + \frac{1}{\alpha} x f'(x) \right) = \frac{G\rho_0^2}{\xi} \frac{1}{x^2} \frac{d}{dx} \left\{ x^2 \left( f'(x) + \frac{1}{x^2} f(x) \int_0^x f(x') 4\pi x'^2 dx' \right) \right\}.$$

Assuming that such a scaling exists implies that  $(\xi/G\rho_0^2)(d\rho_0/dt)$  is a constant that we arbitrarily set to be equal to 1. This leads to

$$(83) \quad \rho_0(t) = \frac{\xi}{G} (t_{coll} - t)^{-1}.$$

so that the central density becomes infinite in a finite time  $t_{coll}$ . Since the collapse time appears as an integration constant, its precise value cannot be explicitly determined. The scaling equation now reads

$$(84) \quad f(x) + \frac{1}{\alpha} x f'(x) = \frac{1}{x^2} \frac{d}{dx} \left\{ x^2 \left( f'(x) + \frac{1}{x^2} f(x) \int_0^x f(x') 4\pi x'^2 dx' \right) \right\},$$

which determines the invariant profile  $f(x)$ . Alternative form of Eq. (84) are given in Appendix A. If one knows the value of  $\alpha$ , Eq. (84) leads to a “shooting problem” where the value of  $f(0)$  is uniquely selected by the requirement of a reasonable large  $x$  behavior for  $f(x)$  at large distances (see below). As  $f(x) \rightarrow 0$  when  $x \rightarrow +\infty$ , we can only keep the leading terms in Eq. (84), which leads to

$$(85) \quad f(x) \sim x^{-\alpha}, \quad \text{when } x \rightarrow +\infty.$$

Finally, the velocity profile as defined by Eq. (52) can be written

$$(86) \quad u(r, t) = -v_0(t) V \left( \frac{r}{r_0(t)} \right),$$

with

$$(87) \quad v_0(t) = \frac{T}{\xi r_0} \quad \text{and} \quad V(x) = \frac{f'(x)}{f(x)} + \frac{4\pi}{x^2} \int_0^x f(x') x'^2 dx'.$$

The invariant profile  $V(x)$  has the asymptotic behaviors

$$(88) \quad V(x) \sim x \quad (x \rightarrow 0), \quad V(x) \sim \frac{1}{x} \quad (x \rightarrow +\infty).$$

## 4.2 Canonical ensemble

In the canonical ensemble in which the temperature  $T$  is a constant, Eq. (78) leads to <sup>1</sup>:

$$(89) \quad \alpha = 2.$$

---

<sup>1</sup>The particular case  $T = 0$  is treated in Appendix B

In that case, the scaling equation (84) can be solved analytically (see Appendix A) and the invariant profile is exactly given by

$$(90) \quad f(x) = \frac{1}{4\pi} \frac{6+x^2}{\left(1+\frac{x^2}{2}\right)^2}.$$

This solution satisfies

$$(91) \quad f(0) = \frac{3}{2\pi} \quad \text{and} \quad f(x) \sim \frac{1}{\pi x^2} \quad (x \rightarrow +\infty).$$

From the first relation and Eq. (83), we find that the central density evolves with time as

$$(92) \quad \rho(0, t) = \rho_0(t) f(0) = \frac{3\xi}{2\pi G} (t_{coll} - t)^{-1},$$

and the core radius as

$$(93) \quad r_0(t) = \left(\frac{T}{\xi}\right)^{1/2} (t_{coll} - t)^{1/2}.$$

On the other hand, using Eq. (90), we find that the velocity profile (87) is given by:

$$(94) \quad v_0(t) = \left(\frac{T}{\xi}\right)^{1/2} (t_{coll} - t)^{-1/2} \quad \text{and} \quad V(x) = \frac{2x}{6+x^2}.$$

At  $t = t_{coll}$ , the scaling solutions (78) and (86) converge to the singular profiles

$$(95) \quad \rho(r, t = t_{coll}) = \frac{T}{\pi G r^2}, \quad u(r, t = t_{coll}) = -\frac{2T}{\xi r}.$$

It is interesting to note that the density profile (95) has the same  $r$ -dependence as that of the singular solution (30) to the static isothermal gas sphere, the two profiles just differing by a factor of 2. Therefore, the relationship between the density and the gravitational potential in the tail of the scaling profile is given by a Boltzmann distribution

$$(96) \quad \rho \sim A e^{-\frac{1}{2T}\Phi},$$

with a temperature  $2T$  instead of  $T$ . The  $r^{-2}$  decay of the density at large distances was also found by Penston [40] in his investigation of the self-similar collapse of isothermal gas spheres described by fluid equations. This is probably a general characteristic of the collapse in the canonical ensemble ( $T = \text{Cst.}$ ). It should be noticed that the free energy (44) does not diverge although the system undergoes a complete collapse.

We now show that the self-similar solution (78) is not sufficient to quantitatively describe the full density profile (especially when  $r \sim R$ ). To understand the problem, let us calculate the mass contained in the density profile at  $t = t_{coll}$ . Using Eq. (95), we have

$$(97) \quad M_{scaling} = \int_0^R \frac{T}{\pi G r^2} 4\pi r^2 dr = \frac{4R}{G\beta}.$$

The mass  $M_{scaling}$  is finite but, in general, it is not equal to the total mass  $M$  imposed by the initial condition. This means that there must be a non-scaling contribution to the density which should contain the remaining mass (possibly negative when  $M < M_{scaling}$ , i.e.  $\eta < 4$ ).

That the scaling solution (78) is not an exact solution of our problem is also visible from the boundary conditions. Indeed, according to Eq. (62) we should have

$$(98) \quad \frac{\partial \ln \rho}{\partial r} = -\frac{\beta GM}{R^2}, \quad \text{for} \quad r = R.$$

This relation is clearly not satisfied by Eq. (95) except for the particular value  $\eta = 2$ . These problems originate because we work in a finite container. The scaling solution (78) would be correct in an infinite domain but, in that case, the total mass of the system is infinite. In addition, if we remove the box, the isothermal spheres are always unstable and the interesting bifurcations between “equilibrium” and “collapsed” states described in section 2 are lost.

Strictly speaking, we expect that the self-similar solution (78) will describe the density behavior in the scaling limit defined by

$$(99) \quad t \rightarrow t_{coll} \quad \text{or} \quad r_0 \rightarrow 0, \quad \text{and} \quad x = r/r_0 \quad \text{fixed.}$$

For the reasons indicated above, it probably does not reproduce the density near the edge of the box, that is for  $r \sim R \gg r_0$ . Therefore, we write another equation for the density, making the following *ansatz*:

$$(100) \quad \rho(r, t) = \rho_0(t) f\left(\frac{r}{r_0(t)}\right) + \frac{T}{4\pi G} F(r, t),$$

where  $F(r, t)$  is the profile that contains the excess or deficit of mass. For  $t = t_{coll}$ , we have

$$(101) \quad \rho(r, t_{coll}) = \frac{T}{4\pi G} \left( \frac{4}{r^2} + F(r) \right),$$

and it would be desirable to find an approximate expression for the function  $F(r) = F(r, t_{coll})$ . A differential equation for  $F(r)$  can be obtained by substituting the *ansatz* (100) in the dynamical equation (77) and taking the limit  $t = t_{coll}$ . We need first to discuss the term  $\partial\rho/\partial t(r, t_{coll})$ . For  $t \rightarrow t_{coll}$ , we can use the expansion of the function  $f(x)$ , given by Eq. (90), to second order in  $1/x^2$  to get

$$(102) \quad \rho(r, t) = \frac{\rho_0 r_0^2}{\pi r^2} \left( 1 + \frac{2r_0^2}{r^2} + \dots \right) + \frac{T}{4\pi G} F(r, t).$$

Then, using Eqs. (78) and (83), we obtain to first order in  $t_{coll} - t$ :

$$(103) \quad \rho(r, t) = \rho(r, t_{coll}) + \frac{T^2}{4\pi G \xi} \left[ \frac{8}{r^4} - \frac{\xi}{T} \frac{\partial F}{\partial t}(r, t_{coll}) \right] (t_{coll} - t) + \dots$$

leading to

$$(104) \quad \frac{\partial \rho}{\partial t}(r, t_{coll}) = \frac{T^2}{4\pi G \xi} \left[ -\frac{8}{r^4} + \frac{\xi}{T} \frac{\partial F}{\partial t}(r, t_{coll}) \right].$$

The trouble is that we do not know the exact expression for  $\partial F/\partial t(r, t_{coll})$ . It is possible, however, to derive an exact integral equation that it must satisfy. Since the exact profile  $\rho(r, t)$  conserves mass, we have

$$(105) \quad \int_0^R \frac{\partial \rho}{\partial t}(r, t_{coll}) r^2 dr = 0.$$

The scaling profile  $\rho_{scaling}(r, t)$  is an exact solution of Eq. (77) but it does not conserve mass. Multiplying Eq. (77) by  $r^2$  and integrating from  $r = 0$  to  $R$ , we get

$$(106) \quad \int_0^R \frac{\partial \rho_{scaling}}{\partial t}(r, t_{coll}) r^2 dr = \frac{R^2}{\xi} \left( T \frac{\partial \rho_{scaling}}{\partial r}(R) + \rho_{scaling} \frac{GM_{scaling}}{R^2} \right)_{|t=t_{coll}} = \frac{2T^2}{\pi G \xi R},$$

where we have used Eqs. (95) and (97) to obtain the last equality. Now, subtracting Eqs. (105) and (106) and using Eq. (100), we find that

$$(107) \quad \int_0^R \frac{\partial F}{\partial t}(r, t_{coll}) r^2 dr = -\frac{8T}{\xi R}.$$

This relation implies in particular that we cannot take  $(\partial F / \partial t)(r, t_{coll}) = 0$  in Eq. (104). In fact, it is likely that  $F(r, t)$  involves combinations of the type

$$(108) \quad F(r, t) \sim \rho_0 f(r/r_0) r^2 F(r), \quad \frac{1}{r^2} (r^2 + cr_0^2) F(r), \quad F(\sqrt{r^2 + cr_0^2}), \dots$$

which reduce to  $F(r)$  in the limit  $t \rightarrow t_{coll}$ . Considering the time derivative of these expressions at  $t = t_{coll}$ , we find that they take only one of the two forms  $F(r)/r^2$  and  $F'(r)/r$ . We are therefore led to make the following *ansatz* :

$$(109) \quad \frac{\xi}{T} \frac{\partial F}{\partial t}(r, t_{coll}) = a \frac{F(r)}{r^2} + b \frac{F'(r)}{r},$$

where  $a$  and  $b$  are some unknown constants which will be determined by an optimization procedure (see below). If we substitute the *ansatz* (100) in Eq. (77), take the limit  $t = t_{coll}$  and use Eqs. (104)- (109), we find after some simplifications that  $F(r)$  satisfies the differential equation

$$(110) \quad r^2 F'' + (6 - b)r F' + r^2 F^2 + (8 - a)F + F' \int_0^r F(x) x^2 dx - \frac{8}{r^3} \int_0^r F(x) x^2 dx = 0.$$

Interestingly, the final profile equation (110) is *not* obtained by setting  $\partial \rho / \partial t = 0$  in the dynamical equation as, even in the stationary looking tail,  $\partial \rho / \partial t$  is in fact of order 1 due to the fast collapse dynamics.

Eq. (110) leads to another “shooting problem”, starting this time from  $r = R$ . The value  $F(R)$  is selected by imposing the condition that the total mass is  $M$ . This yields

$$(111) \quad \int_0^R F(r) r^2 dr = \beta G \left( M - \frac{4R}{\beta G} \right),$$

where  $4R/\beta G = M_{scaling}$  is the mass included in the scaling part. Moreover,  $F'(R)$  is fully determined by the boundary condition (62) at  $r = R$  which implies, together with Eq. (101),

$$(112) \quad F'(R) + \frac{\beta GM}{R^2} F(R) = \frac{8}{R^3} - \frac{4\beta GM}{R^4}.$$

Finally, the exact relation (107) combined with Eq. (109) imposes the condition

$$(113) \quad (a - b) \int_0^R F(r) dr + bRF(R) = -\frac{8}{R}.$$

In order to determine the values of  $a$  and  $b$  we shall require that the value of the total density at  $r = R$  is maximum, as the system would certainly tend to expel some mass if it were not bound to a sphere (recall that the profile  $F$  arises because of boundary effects). In addition, Eq. (113) implies that  $F$  is integrable, so that the optimization process should be performed including this constraint (if  $F$  is integrable, then Eq. (113) is automatically satisfied as it is equivalent to the conservation of mass). In the section devoted to numerical simulations, we study  $F$  numerically and compare it with the numerical profiles obtained by simulating the full dynamical equations.

### 4.3 Microcanonical ensemble

If the temperature is not fixed but determined by the energy constraint (54), then the exponent  $\alpha$  is not known *a priori*. However, we have solved Eq. (84) numerically for different values of  $\alpha$  and found that there is a maximum value for  $\alpha$  above which Eq. (84) does not have any physical solutions. This value,

$$(114) \quad \alpha_{max} = 2.2097330356\dots$$

is extremely close (if not identical) to that found by Lynden-Bell & Eggleton [26] in their investigation on the gravitational collapse of globular clusters using fluid equations (a similar value is found by Cohn [25] using orbit averaged Fokker-Planck equations and, to some extent, by Larson [24] using moment equations). This agreement was unexpected because our relaxation equation differs from those of Refs. [26, 25, 24], as discussed in section 3.2. However, this coincidence may suggest that the intrinsic exponent characterizing the self-similar collapse of self-gravitating systems is in some sense “universal” provided that some general properties are satisfied by the dynamical equations (in particular the first and second principles of thermodynamics). For example, if the temperature is held constant (canonical ensemble) then  $\alpha = 2$  while if it is allowed to diverge (microcanonical ensemble) then  $\alpha \simeq 2.21$ .

In the present case,  $\alpha_{max}$  is just an upper bound on  $\alpha$  not a unique eigenvalue determined by the scaling equations like in Ref. [26]. However, this maximum value leads to the fastest divergence of the entropy and the temperature so it is expected to be dynamically selected by the maximum entropy production principle. Indeed, the temperature and the entropy respectively diverge like

$$(115) \quad T(t) \sim (t_{coll} - t)^{-\frac{\alpha-2}{\alpha}}, \quad S(t) \sim -\frac{3(\alpha-2)}{2\alpha} \ln(t_{coll} - t).$$

Note that these divergences are quite weak as the exponent involved is small

$$(116) \quad \frac{\alpha-2}{\alpha} = 0.094913291\dots \quad \text{for } \alpha = \alpha_{max}.$$

For  $\alpha = \alpha_{max}$ , the value of  $f(0)$  selected by the shooting problem defined by Eq. (84) is  $f(0) = 5.178\dots$ . Therefore, the central density evolves with time as

$$(117) \quad \rho(0, t) = 5.178\dots \frac{\xi}{G} (t_{coll} - t)^{-1}.$$

The coefficient in front of  $(t_{coll} - t)^{-1}$  is approximately 10 times larger than for  $\alpha = 2$  (see Eq. (92)). Using Eq. (81), we find that the core radius decreases to zero as:

$$(118) \quad r_0(t) \sim (t_{coll} - t)^{1/\alpha}.$$

The density profile at  $t = t_{coll}$  is equal to

$$(119) \quad \rho(r, t = t_{coll}) = \frac{K}{r^\alpha}.$$

where  $K$  is an undetermined constant. Using Eq. (119) and the Gauss theorem (61), we find that the relation between  $\rho$  and  $\Phi$  in the tail of the self-similar profile is that of a *polytrope*:

$$(120) \quad \rho \sim (\Phi - Cst.)^{\frac{\alpha}{\alpha-2}},$$

with index  $n = \alpha/(\alpha - 2) \simeq 10.53$ .

We now address the divergence of the potential energy which should match that of the temperature (or kinetic energy) in order to ensure energy conservation. After an integration by parts, the potential energy can be written

$$(121) \quad W = -\frac{GM^2}{2R} - \frac{1}{8\pi G} \int (\nabla \Phi)^2 d^3 \mathbf{r}.$$

Then, using the Gauss theorem, we obtain

$$(122) \quad W = -\frac{GM^2}{2R} - \frac{G}{2} \int_0^R \frac{1}{r^2} \left( \int_0^r \rho(r') 4\pi r'^2 dr' \right)^2 dr.$$

If we assume that all the potential energy is in the scaling profile we get a contradiction since

$$(123) \quad W_{scaling}(t = t_{coll}) \sim -\frac{G}{2} \int_0^R \frac{1}{r^2} \left( \int_0^r \frac{1}{r'^\alpha} 4\pi r'^2 dr' \right)^2 dr \sim - \int_0^R r^{4-2\alpha} dr,$$

converges for  $\alpha < 5/2$ . Since the temperature diverges with time for  $\alpha = \alpha_{max}$ , the total energy cannot be conserved. This would suggest that  $\alpha = 2$  like in the microcanonical ensemble. We cannot rigorously exclude this possibility but a value of  $\alpha$  close to  $\alpha_{max} \simeq 2.21$  is more consistent with the numerical simulations (see section 5) and leads to a larger increase of entropy (in agreement with our maximum entropy production principle). If this value is correct, the divergence of the gravitational energy should originate from the non scaling part of the profile (which also accommodates for the mass conservation). In the following, a possible scenario allowing for the gravitational energy to diverge is presented.

Let us assume that there exists two length scales  $r_1$  and  $r_2$  satisfying

$$(124) \quad r_0 \ll r_1 \ll r_2 \ll R,$$

with  $r_0, r_1, r_2 \rightarrow 0$  for  $t \rightarrow t_{coll}$  such that the mass between  $r_1$  and  $r_2$  is of order 1. The physical picture that we have in mind is that this mass will progress towards the center of the domain and form a dense nucleus with larger and larger potential energy. We assume that for  $r_1 < r < r_2$  the density behaves as

$$(125) \quad \rho(r, t) \sim \frac{r_1^{\gamma-\alpha}}{r^\gamma},$$

so that this functional form matches with the scaling profile for  $r \sim r_1$ . If we impose that the total mass between  $r_1$  and  $r_2$  is of order 1, we get

$$(126) \quad \int_{r_1}^{r_2} \frac{r_1^{\gamma-\alpha}}{r^\gamma} r^2 dr \sim 1 \quad \text{i.e.} \quad r_2 \sim r_1^{\frac{\alpha-\gamma}{3-\gamma}},$$

which shows that  $r_2 \gg r_1$  since  $\alpha < 3$ . Now, the contribution to the potential energy of the density between  $r_1$  and  $r_2$  which is assumed to be the dominant part is

$$(127) \quad W \sim - \int_{r_1}^{r_2} \frac{1}{r^2} \left( \int_{r_1}^r \frac{r_1^{\gamma-\alpha}}{r'^\gamma} r'^2 dr' \right)^2 dr \sim -r_1^{2(\gamma-\alpha)} r_2^{5-2\gamma} \sim -r_1^{-(\alpha-\gamma)/(3-\gamma)},$$

where we have used Eq. (126) to get the last equivalent. Since the divergence of the potential energy must compensate that of the kinetic term we must have

$$(128) \quad -W \sim \frac{3}{2} MT \sim r_0^{2-\alpha},$$

where we have used Eqs. (78)(81) to get the last equivalent. This relation implies that  $r_0$  and  $r_1$  are related by:

$$(129) \quad r_1 \sim r_0^{(\alpha-2)(3-\gamma)/(\alpha-\gamma)}.$$

Now, imposing  $r_1 \gg r_0$  leads to

$$(130) \quad \gamma < 2.$$

Therefore, any value of  $\gamma < 2$  leads to the correct divergence of  $W$  within this scenario. Note that Eq. (125) may arise from the next correction to scaling of the form

$$(131) \quad \rho(r, t) = \rho_0 f(r/r_0) + \rho_0^{\bar{\gamma}} f_1(r/r_0) + \dots$$

with  $f_1(x) \sim x^{-\gamma}$  for large  $x$  and  $\bar{\gamma} < 1$  for the first term to be dominant in the scaling regime. Matching the large  $x$  behavior of Eqs. (125) and (131) we obtain

$$(132) \quad \rho_0^{\bar{\gamma}} r_0^\gamma \sim r_1^{\gamma-\alpha},$$

which is equivalent to

$$(133) \quad r_1 \sim r_0^{\frac{\alpha\bar{\gamma}-\gamma}{\alpha-\gamma}}.$$

Since  $\bar{\gamma} < 1$  this implies that  $r_1 \gg r_0$  as expected. More precisely, comparing with Eq. (129) we have

$$(134) \quad \bar{\gamma} = \frac{\gamma + (\alpha - 2)(3 - \gamma)}{\alpha},$$

and we check that the condition  $\gamma < 2$  is equivalent to  $\bar{\gamma} < 1$ .

#### 4.4 Analogy with critical phenomena

In this section, we try to determine the domain of validity of the scaling regime by using an analogy with the theory of critical phenomena. For simplicity, we work in the canonical ensemble but we expect to get similar results in the microcanonical ensemble. For  $\eta = \theta^{-1} = \beta GM/R$  close to  $\eta_c$ , we define

$$(135) \quad \epsilon = \frac{|\eta - \eta_c|}{\eta_c} \sim \frac{|\theta_c - \theta|}{\theta_c} \ll 1.$$

For  $\eta = \eta_c$  the central density  $\rho(0, t)$  goes to a finite constant  $\rho_\infty$  when  $t \rightarrow +\infty$ . Writing  $\delta\rho(t) = \rho_\infty - \rho(0, t)$  and using Eq. (56), which is quadratic in  $\rho$ , we argue that, for  $\eta \leq \eta_c$ ,  $\delta\rho(t)$  satisfies an equation of the form

$$(136) \quad \frac{d\delta\rho}{dt} \sim \frac{\delta\rho}{\tau} - \frac{G}{\xi} \delta\rho^2,$$

where  $\tau$  plays the role of a correlation time which is expected to diverge for  $\eta = \eta_c$  leading to a slow (algebraic) convergence of  $\delta\rho$  towards 0 at the critical temperature. Actually, for  $\eta = \eta_c$ , Eq. (136) leads to

$$(137) \quad \delta\rho \sim t^{-1}.$$

Now, if we stand slightly above the critical point ( $\eta > \eta_c$ ), we expect this behavior to hold up to a time of order  $t_{coll}$  for which the perturbation term proportional to  $(1/\xi)(T - T_c)\Delta\rho(0, t) \sim -\epsilon$  is of the same order as  $\partial\rho/\partial t \sim -1/t^2$ . This yields

$$(138) \quad t_{coll} \sim \epsilon^{-1/2} \sim (\eta - \eta_c)^{-1/2}.$$

By analogy with critical phenomena, it is natural to expect that  $\tau$  has the same behavior for  $\eta < \eta_c$ :

$$(139) \quad \tau \sim (\eta_c - \eta)^{-1/2}.$$

Therefore, for  $\eta < \eta_c$  and according to Eq. (136),  $\delta\rho(t)$  tends exponentially rapidly to the equilibrium value

$$(140) \quad \rho_\infty - \rho(0, t = +\infty) = \frac{\xi}{G} \tau^{-1} \sim (\eta_c - \eta)^{1/2}.$$

This relation is consistent with the results obtained in the equilibrium study of Chavanis [18], where the exact result

$$(141) \quad 1 - \frac{\rho(0)}{\rho_\infty} \approx \left[ \frac{8}{\eta_c - 2} \left( 1 - \frac{\eta}{\eta_c} \right) \right]^{1/2}.$$

is derived close to the critical point.

Another interesting question concerns the extent of the scaling regime which we expect to be valid for  $t_{coll} - t < \delta t \sim \epsilon^\nu$ . To compute  $\nu$ , we integrate the dynamical equation in the regime where the perturbation  $-\epsilon\Delta\rho$  dominates:

$$(142) \quad \frac{\partial\rho}{\partial t} \simeq -\epsilon\Delta\rho,$$

leading to

$$(143) \quad \rho(0, t) \sim \int_{k < r_0^{-1}} k^2 \exp(k^2 \epsilon t) dk \sim r_0^{-2} \exp(r_0^{-2} \epsilon t),$$

where we have introduced an upper momentum cut-off of order  $r_0^{-1}$  to prevent the integral from diverging. Indeed, the Laplacian of  $\rho$  should become positive for  $r \gg r_0$  as  $\Delta(r^{-2}) = 2r^{-4} > 0$ . Thus, for  $\epsilon \ll 1$ , we expect that the density will first saturate to  $\rho_\infty$  for a long time of order  $t_{coll}$  [see Eq. (137)], before rapidly increasing [see Eq. (143)], and ultimately reaching the scaling regime [see Eq. (78)]. Comparing Eq. (143) with the density in the scaling regime  $\rho(0, t) \sim r_0^{-2}$ ,

we find that the scaling regime is reached at a time  $t_*$  such that  $r_0^{-2}\epsilon t_* \sim 1$  (for the argument in the exponential to be of order 1). Since  $r_0 \sim (t_{coll} - t)^{1/2}$  in the scaling regime, we get  $t_{coll} - t_* \sim \epsilon t_{coll}$ . Therefore, the width of the scaling regime,  $\delta t = t_{coll} - t_*$ , behaves like

$$(144) \quad \delta t \sim t_{coll}\epsilon \sim \epsilon^{1/2},$$

establishing  $\nu = 1/2$ . Close to the critical point, the collapse occurs at a very late time and the width of the scaling regime is very small. We therefore expect our results of sections 4.1-4.3 to be all the more valid far from the critical point.

Regrouping all these results, and using again an analogy with critical phenomena, we expect that the central density obeys the following equation

$$(145) \quad \rho(0, t) = (t_{coll} - t)^{-1}G(t_{coll}(t_{coll} - t)),$$

where  $t_{coll} \sim \epsilon^{-1/2}$  and the scaling function  $G$  satisfies

$$(146) \quad G(0) = \frac{3}{2\pi}, \quad G(x) \sim \rho_\infty \sqrt{x}, \quad \text{for } x \rightarrow +\infty.$$

## 5 Numerical simulations

We now perform direct numerical simulations of Eq. (56) and compare with the theoretical results of sections 3.3 and 4. The numerical algorithm used to solve the relaxation equation is described in Rosier (in preparation).

### 5.1 Dimensionless variables

It is convenient to normalize distances by the box radius  $R$ , densities by the average density  $M/R^3$ , and time by a dynamical time defined as  $\xi R^3/GM$ . More specifically, we set

$$(147) \quad \mathbf{x} = \frac{\mathbf{r}}{R}, \quad n = \frac{\rho}{(M/R^3)}, \quad \psi = \frac{\Phi}{(GM/R)}, \quad \tau = \frac{t}{\left(\frac{\xi R^3}{GM}\right)}.$$

We also recall that the dimensionless energy and temperature are denoted by

$$(148) \quad \Lambda = -\frac{ER}{GM^2}, \quad \theta = \eta^{-1} = \frac{TR}{GM}.$$

Using these dimensionless quantities, our system of equations can be rewritten

$$(149) \quad \frac{\partial n}{\partial t} = \nabla(\theta \nabla n + n \nabla \psi),$$

$$(150) \quad \Delta \psi = 4\pi n,$$

$$(151) \quad -\Lambda = \frac{3}{2}\theta + \frac{1}{2} \int n\psi \, d^3\mathbf{x},$$

with boundary conditions

$$(152) \quad \frac{\partial \psi}{\partial x}(0) = 0, \quad \psi(1) = -1, \quad \theta \frac{\partial n}{\partial x}(1) + n(1) = 0.$$

These equations have to be solved in a ball of radius  $|\mathbf{x}| = 1$ . Under this form, it is clear that the evolution of the system depends on a single control parameter  $\Lambda$  (in the microcanonical ensemble) or  $\theta$  (in the canonical ensemble). Introducing dimensionless variables is equivalent to taking  $M = R = G = \xi = 1$  and  $E = -\Lambda$ ,  $T = \theta$  in the original equations and we have taken this convention in the numerical simulations.

In most of our numerical experiments, we have started from a homogeneous sphere with radius  $R$  and density

$$(153) \quad \rho_* = \frac{3M}{4\pi R^3}.$$

This configuration has a potential energy  $W_0 = -\frac{3GM^2}{5R}$ . In the canonical ensemble the temperature is equal to  $T$  at any time. In the microcanonical ensemble, the initial temperature  $T_0$  is adjusted in order to have the desired value of

$$(154) \quad \Lambda \equiv -\frac{ER}{GM^2} = \frac{3}{5} - \frac{3RT_0}{2GM}.$$

By changing  $T$  or  $E$  we can explore the whole bifurcation diagram of Figs. 1- 2 and check the theoretical predictions of sections 2-4.

## 5.2 Microcanonical ensemble

When the energy  $E$  is fixed (microcanonical description), we obtain the following results:

**Result 1:** (i) When  $\Lambda < \Lambda_c = 0.3345\dots$ , the system settles down to a local entropy maximum. (ii) When  $\Lambda > \Lambda_c$ , the system undergoes a gravitational collapse (gravothermal catastrophe).

For  $\Lambda = 0.334 < \Lambda_c$ , the quantities  $\rho(0, t)$ ,  $T(t)$ ,  $r_K(t)$  and  $S(t)$  converge to finite values and the system settles down to a stable thermodynamical equilibrium (Fig. 5). The equilibrium profile is smooth with a density contrast  $\mathcal{R} \simeq 596$  less than the critical value  $\sim 709$  found by Antonov. At large distances, the density decays like  $r^{-2}$  (Fig. 6) like the singular sphere (see section. 2.4).

For  $\Lambda = 0.359 > \Lambda_c$ , the behavior of the system is completely different:  $\rho(0, t)$  and  $T(t)$  diverge to  $+\infty$  and  $r_K(t)$  goes to zero in a finite time  $t_{coll}$  (Fig. 7). We were able to follow this “gravothermal catastrophe” up to a density contrast  $\mathcal{R} \sim 10^4$ . The entropy  $S(t)$  also diverges to  $+\infty$ , but the evolution is slower (logarithmic). For  $\Lambda = 0.335 = \Lambda_c^+$ , the system first tends to converge to an equilibrium state but eventually collapses (Fig. 8).

**Result 2:** The collapse time diverges like  $t_{coll} \sim (\Lambda - \Lambda_c)^{-1/2}$  when we approach the critical point  $\Lambda_c$ .

In Fig. 9, we plot the inverse of the central density as a function of time for different values of  $\Lambda$ . For short times, the density is approximately uniform, as it is initially. In that case, the diffusion term in Eq. (56) cancels out and the system evolves under the influence of the gravitational term alone. Using the Poisson equation (4), the relaxation equation (56) reduces to

$$(155) \quad \frac{d\rho}{dt} = \frac{4\pi G}{\xi} \rho^2.$$

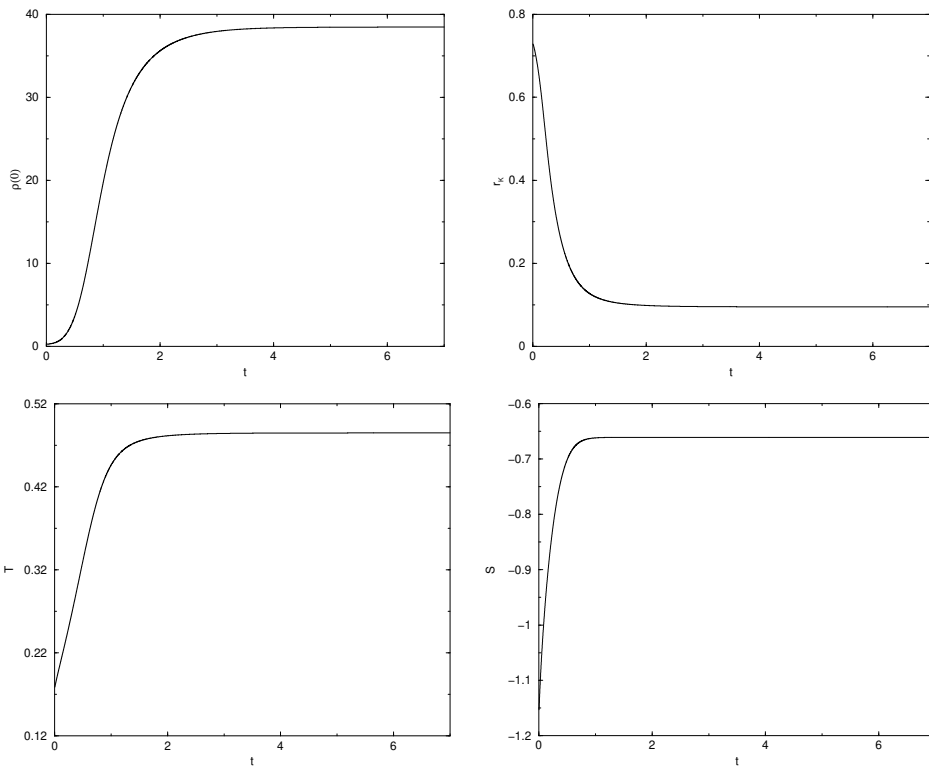


Figure 5: Evolution of central density, King radius, temperature and entropy for  $\Lambda = 0.334 < \Lambda_c$ . The system evolves towards an equilibrium state.

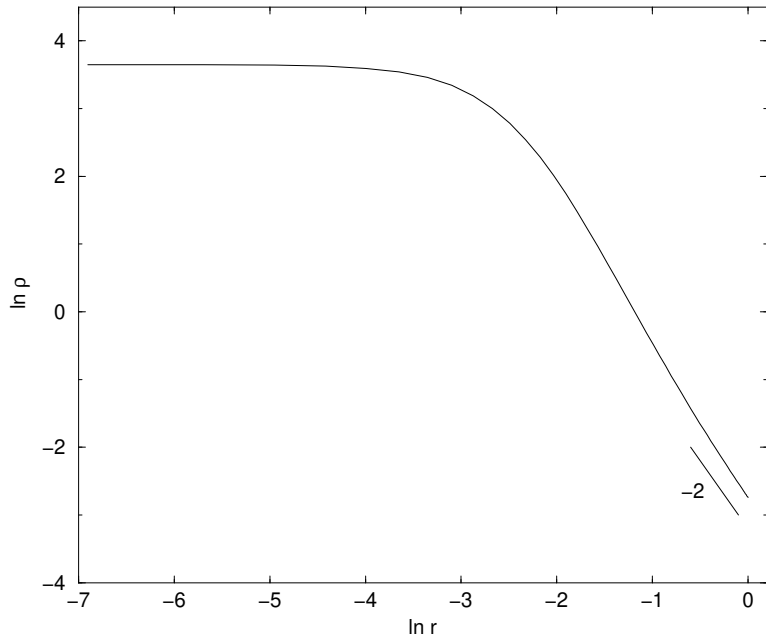


Figure 6: Equilibrium density profile for  $\Lambda = 0.334 < \Lambda_c$ . For large values of  $r$ , the density profile behaves as  $r^{-2}$ , like for the singular sphere.

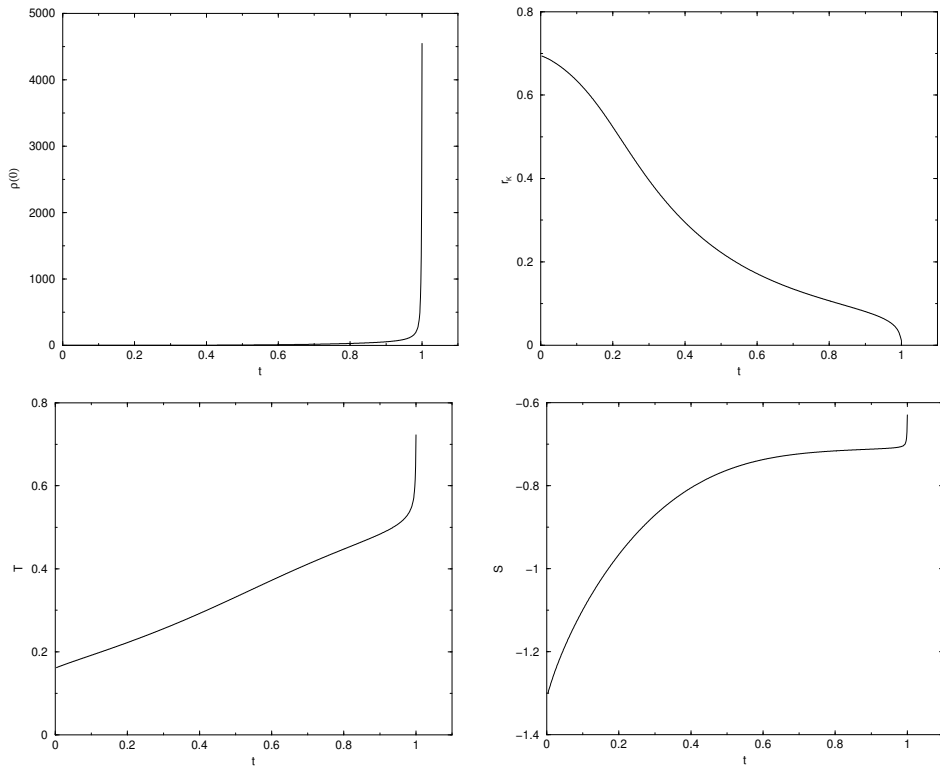


Figure 7: Evolution of central density, King radius, temperature and entropy for  $\Lambda = 0.359 > \Lambda_c$ . The system undergoes a “gravothermal catastrophe” with ever increasing value of entropy.

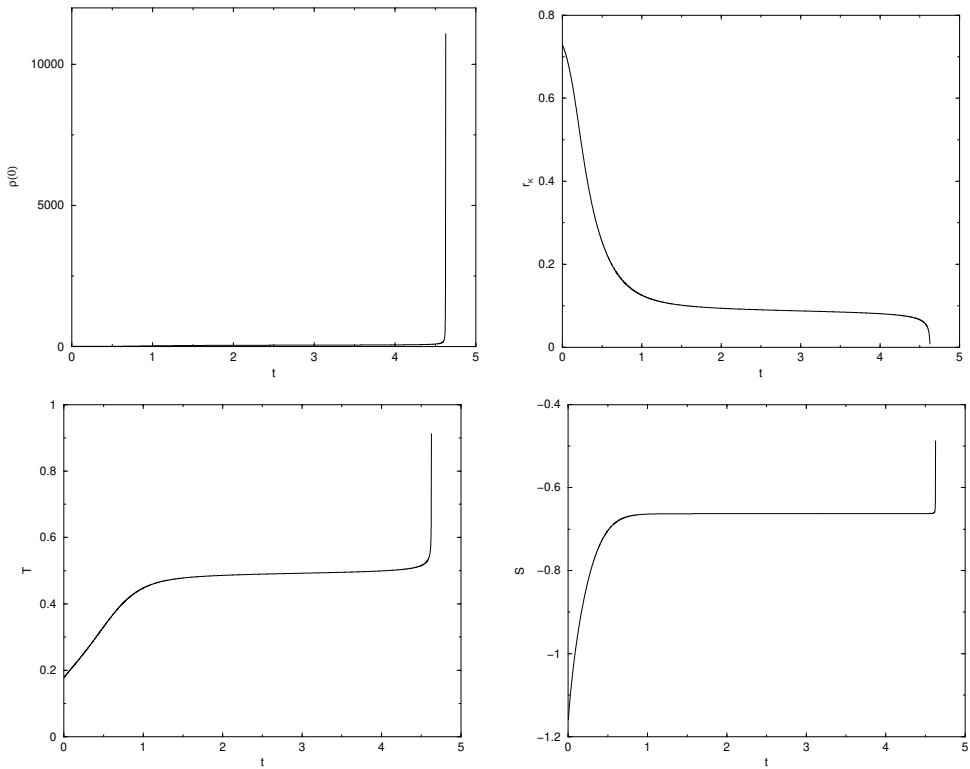


Figure 8: Evolution of central density, King radius, temperature and entropy for  $\Lambda = 0.335 = \Lambda_c^+$ . Close to the critical point, the system first tends to reach a stationary state but finally collapses.

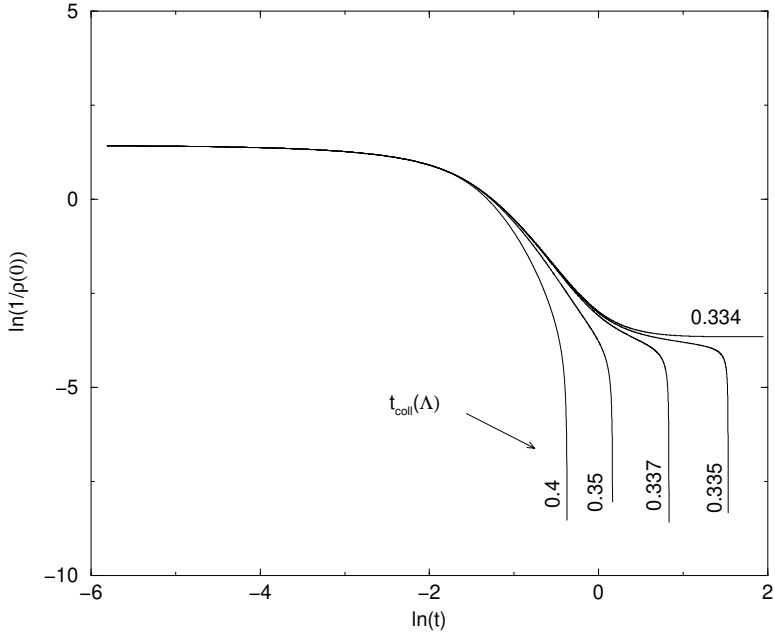


Figure 9: Time evolution of the central density for different values of  $\Lambda$ . The central density  $\rho(0, t)$  becomes infinite in a finite time  $t_{coll}(\Lambda)$  depending on the value of the control parameter  $\Lambda$  (labeling the curves). The figure shows that the collapse time diverges as we approach the critical value  $\Lambda_c = 0.335$  for which a local entropy maximum exists.

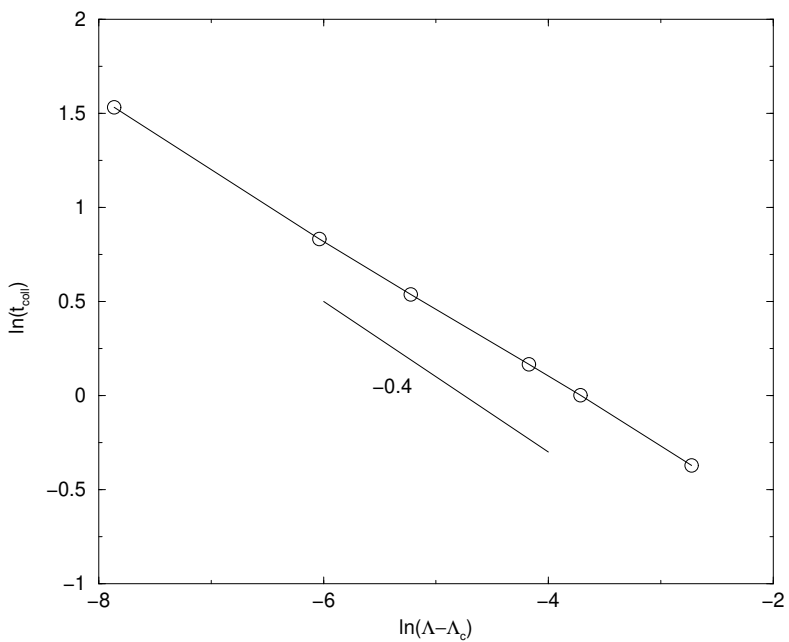


Figure 10: Evolution of the collapse time  $t_{coll}$  with  $\Lambda$ . The figure displays a scaling law  $t_{coll} \sim (\Lambda - \Lambda_c)^{-\delta}$  with  $\delta \simeq 0.4$  close to the theoretical value  $1/2$ .

Solving for  $\rho(t)$ , we get

$$(156) \quad \rho(0, t) = \rho_* \left( 1 + \frac{4\pi G}{\xi} \rho_* t + \dots \right) \quad (t \rightarrow 0),$$

where  $\rho_*$  is the initial density. Over longer time scales, a pressure gradient develops and the two terms in the right hand side of Eq. (56) must be taken into account. The system first reaches a plateau with density  $\sim \rho_\infty$  (corresponding to an approximate balance between pressure and gravity) before gravitational collapse takes place eventually at time  $t_{coll}$ . From Fig. 9, it is seen that the collapse time  $t_{coll}$  clearly depends on the value of  $\Lambda$  and increases as we approach the critical value  $\Lambda_c$ . To be more quantitative, we plot on Fig. 10 the collapse time  $t_{coll}$  as a function of the distance to the critical point  $\Lambda - \Lambda_c$ . A scaling law is observed with an exponent  $\sim -0.4$  close to the predicted value  $-1/2$  (see section 4.4).

**Result 3:** When  $\Lambda > \Lambda_c$ , the collapse proceeds (almost) self-similarly with a scaling exponent  $\alpha = \alpha_{max} \simeq 2.2$ .

During the late stage of the collapse, the density profiles are self-similar that is, they differ only in normalization and scale (Fig. 11). Indeed, if we rescale the density by the central density and the radius by the King radius (79), the density profiles at various times fall on to the same curve (Fig. 12). The invariant profile is compared with the scaling profile  $f(x)$  corresponding to  $\alpha = \alpha_{max}$  and the agreement is excellent, except in the tail. This small discrepancy can be ascribed to the next correction to scaling (see section 4.3) which generates a power law profile between  $r_1$  and  $r_2$  with an index  $\gamma < 2$ . We have checked that the final slope of the profile (corresponding to  $r = R$ ) is equal to  $-\eta$  in agreement with the boundary condition (98). However, this relation only holds on a tiny portion of the curve (invisible on Fig. 12) so that the “effective slope” is more consistent with a value  $\alpha \simeq 2.2$ .

On Fig. 13, we plot the inverse central density as a function of time. It is seen that, for  $t \rightarrow t_{coll}$ , the central density diverges with time like  $(t_{coll} - t)^{-1}$  in good agreement with the theoretical expectation. The slope of the curve on Fig. 13 is approximately  $-0.313$  but is consistently getting closer to the theoretical value  $-1/5.178 \dots \approx -0.193$  corresponding to  $\alpha = \alpha_{max}$  as  $\Lambda$  increases, or as  $t$  approaches  $t_{coll}$  (the small difference is attributed to non scaling corrections, as discussed in section 4.3). Note that a value of  $\alpha = 2$  would yield a much larger slope  $-2\pi/3 \approx -2.094$  (see section 4.2), which is clearly not observed here. Therefore, the simulations are consistent with a value of  $\alpha = \alpha_{max}$ , as expected on physical grounds. This value  $\alpha = \alpha_{max}$  is also consistent with the slow but existing divergence of the temperature. Indeed, the slope of the curve of Fig. 14 is approximately  $-0.1$  in agreement with the prediction (115)(116).

**Result 4:** For  $\Lambda \sim \Lambda_c$ , the density perturbation  $\delta\rho(r, t)/\rho_{eq}(r)$  that triggers the instability presents a “core-halo” structure.

To study the development of the instability we have started from a point on the spiral of Fig. 1 close to  $\Lambda_c$  but with a density contrast  $\mathcal{R} \gtrsim 709$  (more precisely  $\Lambda = 0.3344$  and  $\mathcal{R} = 779$ ). This isothermal sphere, with density profile  $\rho_{eq}(r)$ , is linearly unstable as it is just a critical point of entropy not a true maximum (see sections 2.6 and 3.3). On Fig. 15, we have represented the density perturbation profile  $\delta\rho(r, t)/\rho_{eq}(r) = (\rho(r, t) - \rho_{eq}(r))/\rho_{eq}(r)$  that develops for short times. This density profile presents a “core-halo” structure (i.e. it has two zeros) in excellent agreement with the stability analysis of Padmanabhan [17] (we have computed the exact theoretical profile to compare quantitatively with the simulation).

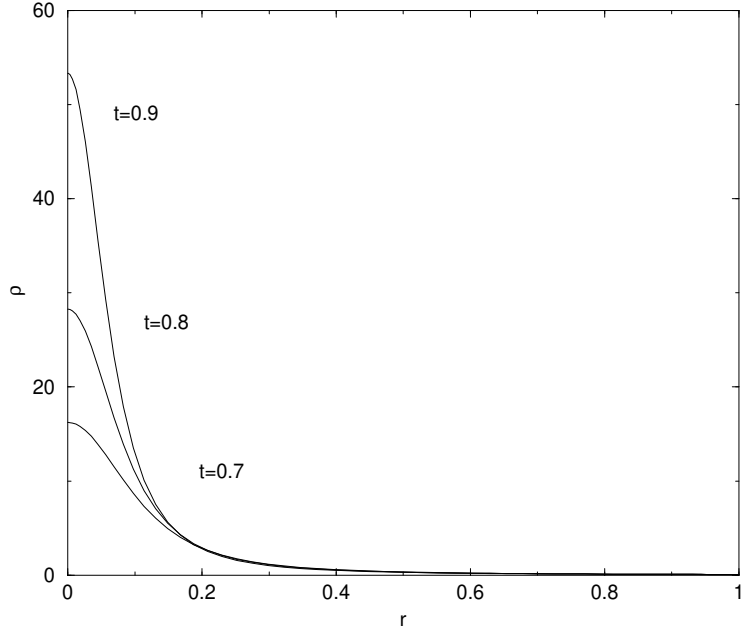


Figure 11: Evolution of the density profile for  $\Lambda = 0.359$  at different times. Starting from a uniform distribution at  $t = 0$ , the system develops a “core-halo” structure with a shrinking core. From this figure, we may suspect that the evolution is self-similar, i.e. the density profiles at different times can be superimposed by an appropriate rescaling.

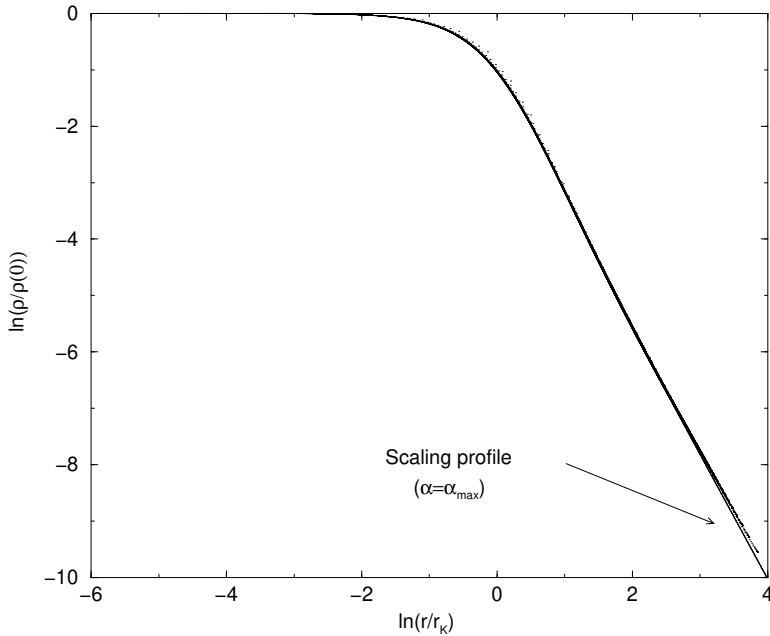


Figure 12: This figure represents the (quasi) invariant density profile obtained for  $\Lambda = 0.359$  by rescaling the density by the central density and the radius by the King radius. It is compared with the theoretical profile  $f(x)$  calculated by solving Eq. (84) with  $\alpha = \alpha_{max}$ .

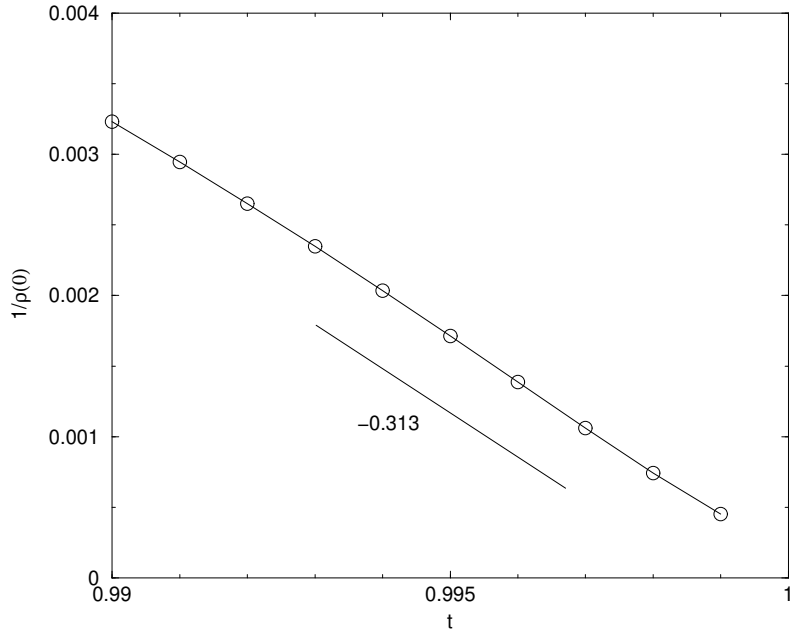


Figure 13: Evolution of the central density for  $\Lambda = 0.359$ . This curve displays a scaling regime  $1/\rho(0, t) = A(t_{coll} - t)$ . The slope of the curve  $A \simeq -0.313$  is of the same order as the theoretical value  $-1/5.178 = -0.193$  corresponding to  $\alpha = \alpha_{max}$ . The small deviation is attributed to non scaling corrections.

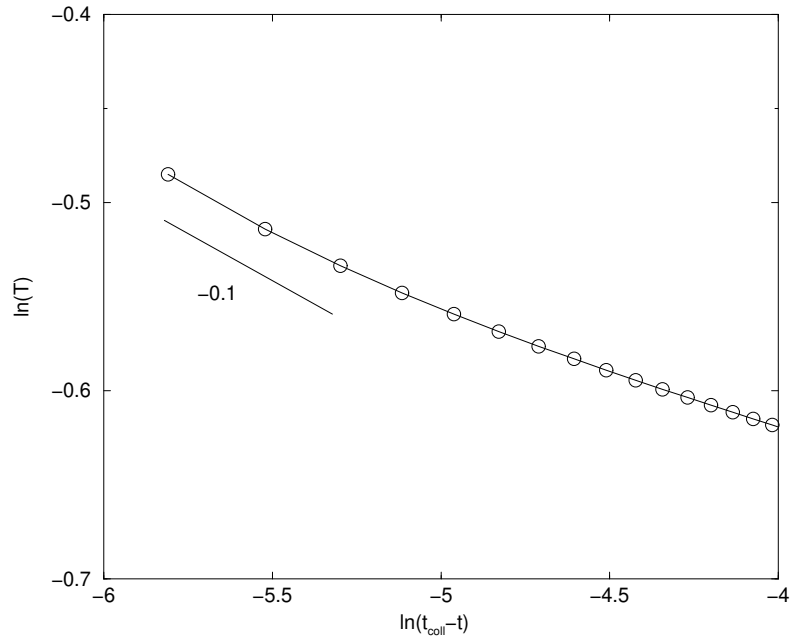


Figure 14: Evolution of the temperature for  $\Lambda = 0.359$ . The curve displays a scaling regime  $T \sim (t_{coll} - t)^{-\gamma}$ . The value of  $\gamma \simeq 0.1$  is in agreement with the theoretical value (116) corresponding to  $\alpha = \alpha_{max}$ .

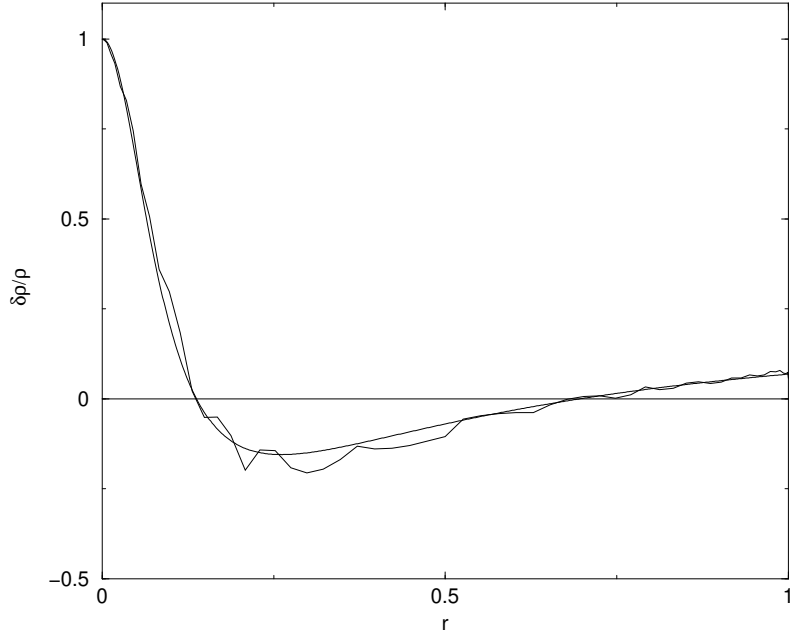


Figure 15: First mode of instability in the microcanonical ensemble. The density profile presents a “core-halo” structure.

### 5.3 Canonical ensemble

When the temperature  $T$  is fixed instead of the energy  $E$ , we find that:

**Result 5:** When  $\eta < \eta_c = 2.517\dots$  the system converges to an equilibrium state while it collapses for  $\eta > \eta_c$  (isothermal collapse). The collapse time diverges like  $t_{coll} \sim (\eta - \eta_c)^{-1/2}$  when we approach the critical point  $\eta_c$ .

In Figs. 16 and 17 we have represented the evolution of  $\rho(0, t)$ ,  $r_K(t)$ ,  $E(t)$  and  $J(t)$  as a function of time. The curves are similar to those obtained in the microcanonical ensemble in equivalent situations. The collapse time  $t_{coll}$  scales with  $\eta - \eta_c$  (see Fig. 18) with an exponent  $\sim -0.6$  close to the theoretical value  $-1/2$ .

**Result 6:** For  $\eta > \eta_c$ , the collapse proceeds (almost) self-similarly with a scaling exponent  $\alpha = 2$ .

In Fig. 19, we plot the scaled density  $\rho(r, t)/\rho(0, t)$  as a function of the scaled distance  $r/r_K(t)$  at different times. The curves tend to superimpose but the thickness of the line indicates that we do not have a strict self-similar regime (in agreement with our theoretical analysis). Indeed, the invariant profile  $f(x)$  computed in section 4.2 matches the numerics very well in the core but does not adequately describes the halo. The difference is due to the non scaling part  $F(r, t)$  that accounts for the mass conservation. In Figs. 20-21, the result of the numerical simulation is compared more precisely with the full theoretical prediction involving the non scaling term. The agreement is excellent throughout the whole domain. In the core, the profile is dominated by the scaling part which implies a  $r^{-2}$  behavior at moderately large distances. As explained previously and in section 4.2, this scaling behavior ceases to be valid near the wall and the contribution of the non scaling part is clearly visible. Its influence on the density profile remains weak but when the density is multiplied by  $r^2$ , this non scaling profile has a non negligible contribution to the total mass.

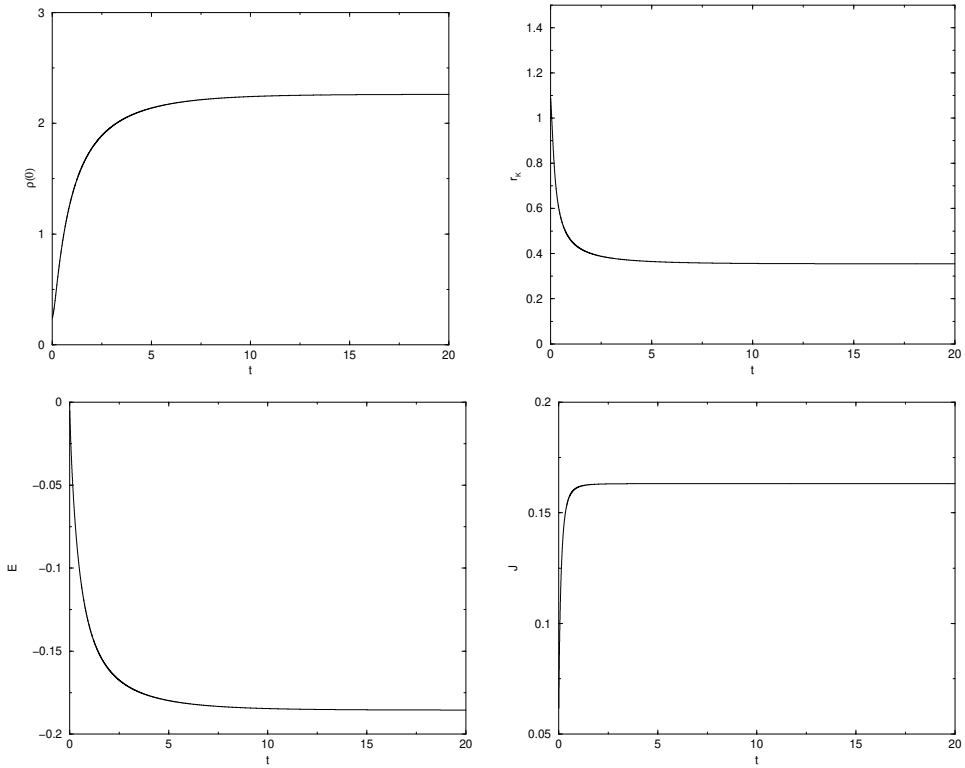


Figure 16: Evolution of central density, King radius, energy and free energy for  $\eta = 2.515 < \eta_c$ . The system evolves towards an equilibrium state.

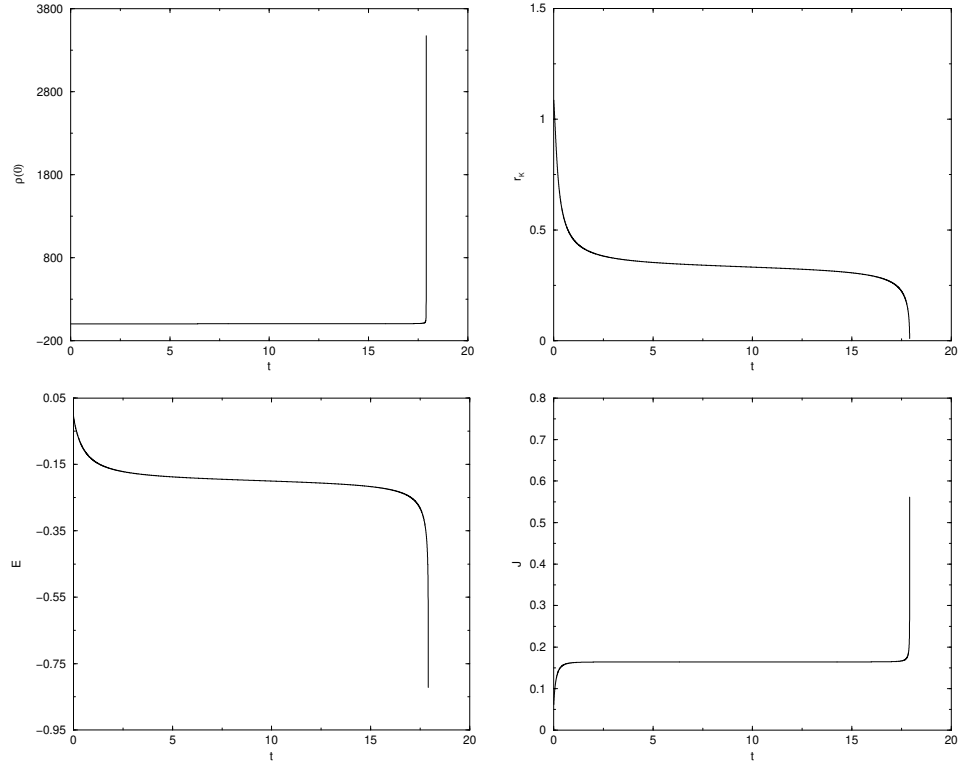


Figure 17: Evolution of central density, King radius, energy and free energy for  $\eta = 2.52 = \eta_c^+$ . The system first tends to reach an equilibrium state but eventually undergoes an isothermal collapse.

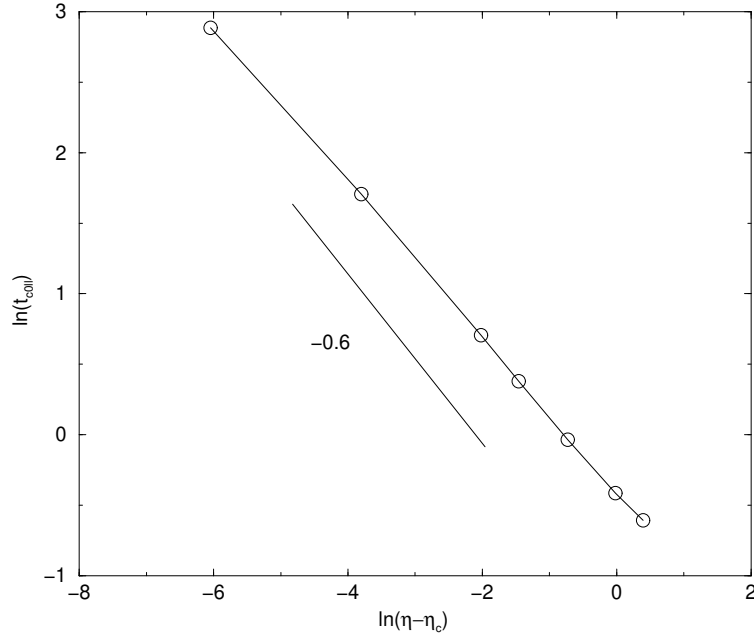


Figure 18: Evolution of the collapse time  $t_{\text{coll}}$  with  $\eta$ . The figure displays a scaling law  $t_{\text{coll}} \sim (\eta - \eta_c)^{-\nu}$  with  $\nu \sim 0.6$  close to the theoretical value  $1/2$ .

In Fig. 22, we see that the central density diverges with time as  $(t_{\text{coll}} - t)^{-1}$ . The slope of the curve is approximately equal to  $-2$  in good agreement with the theoretical prediction  $2\pi/3 \simeq 2.1$  of section 4.2.

**Result 7:** For  $\eta \sim \eta_c$ , the density perturbation  $\delta\rho(r, t)/\rho_{\text{eq}}(r)$  that triggers the instability has only one zero.

In Fig. 23, we study the early development of the instability for  $\eta \sim \eta_c$ . More specifically, we have started the simulations from a point on the spiral of Fig. 2 with  $\eta = 2.510$  and  $\mathcal{R} = 42 \gtrsim 32.1$ . This isothermal sphere is unstable in the canonical ensemble (see sections 2.6 and 3.3) and the perturbation profile that develops for short time is shown in Fig. 23. It is in excellent agreement with the first mode of instability calculated by Chavanis [18] by extending the analysis of Padmanabhan [17] to the canonical ensemble. This profile does *not* present a “core-halo” structure (it has only one zero), in contrast with the first mode of instability in the microcanonical situation. We have also plotted the perturbation profile for an isothermal sphere located near the second extremum of temperature ( $\eta = 1.842\dots$ ) at which a new mode of instability appears [18]. This second mode of instability has a core-halo structure (Fig. 24). Of course, the perturbation profile that develops is a superposition of the first two modes of instability, but we see that its structure is dominated by the contribution of the second mode.

**Result 8:** Isothermal spheres with density contrast  $32.1 \lesssim \mathcal{R} \lesssim 709$  are stable in the microcanonical ensemble and unstable in the canonical ensemble.

To check this prediction, we have started from different isothermal spheres located in the region of negative specific heats (see Fig. 2) where the density contrast is between 32.1 (horizontal tangent) and 709 (vertical tangent). In the first series of experiments, the energy was kept fixed using the constraint (54). In that case, it is found that the spheres are linearly stable, implying that they are local entropy maxima (see section 3.3). However, if the tem-

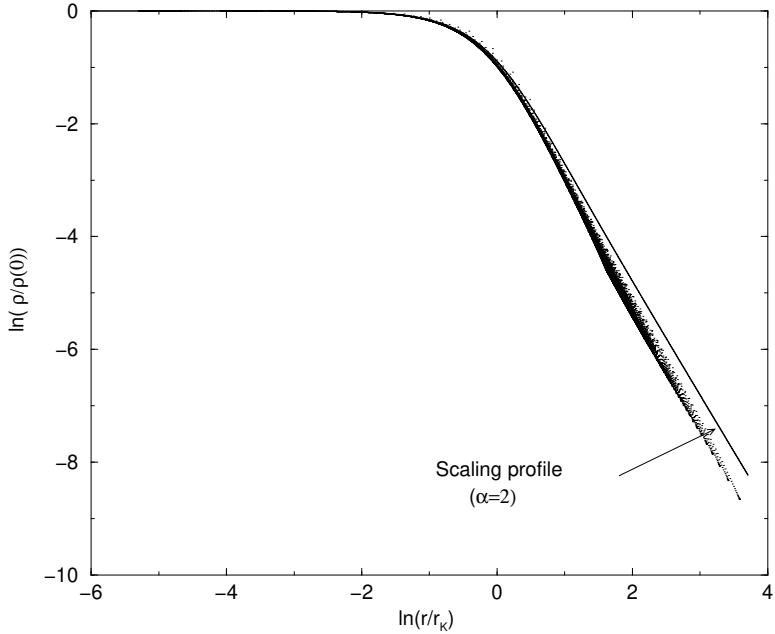


Figure 19: Self-similar profile for  $\eta = 2.75$ . This (quasi) invariant profile is compared with the analytical scaling profile  $f(x)$  with  $\alpha = 2$ . Deviation from the pure scaling law is due to non-scaling corrections that compensate for the excess of mass contained in the scaling profile.

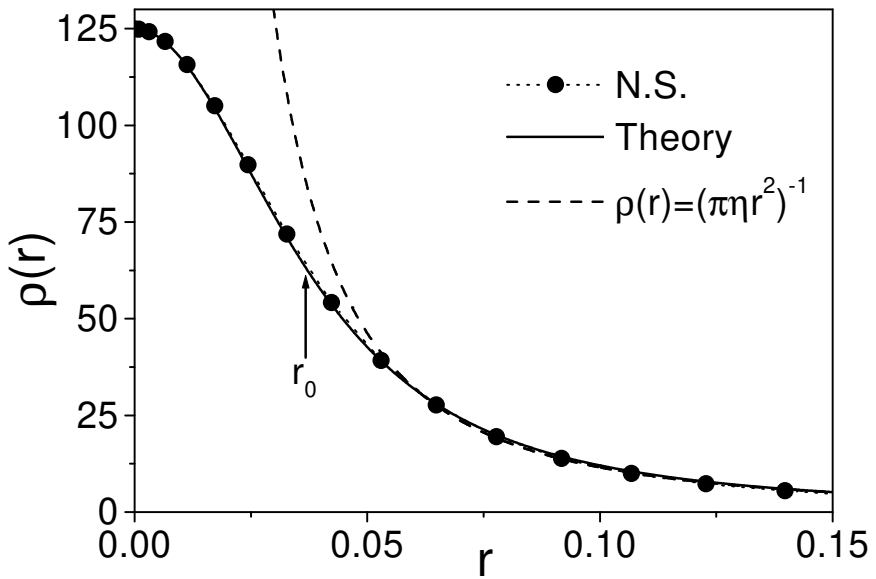


Figure 20: We plot the numerical finite-time density profile for  $\eta = 2.75$  (N.S.), at a time for which the core density is  $\rho(0, t) \approx 124.9 \approx 28.8\rho_\infty$ . This is compared to the exact scaling profile  $\rho_0 f(r/r_0)$  (Theory), with  $f$  given by Eq. (90), and  $\rho_0 = \frac{2\pi}{3}\rho(0, t) \approx 261.6$  and  $r_0 = (\eta\rho_0)^{-1/2} \approx 0.0373$  ( $\rho(r_0, t)/\rho(0, t) = 14/27 \approx 0.519$ ). We also plot the asymptotic density profile,  $\rho_{\text{as}} = (\pi\eta r^2)^{-1}$ , valid for  $r_0 \ll r \ll 1$ . In this region, the correction to scaling is negligible.

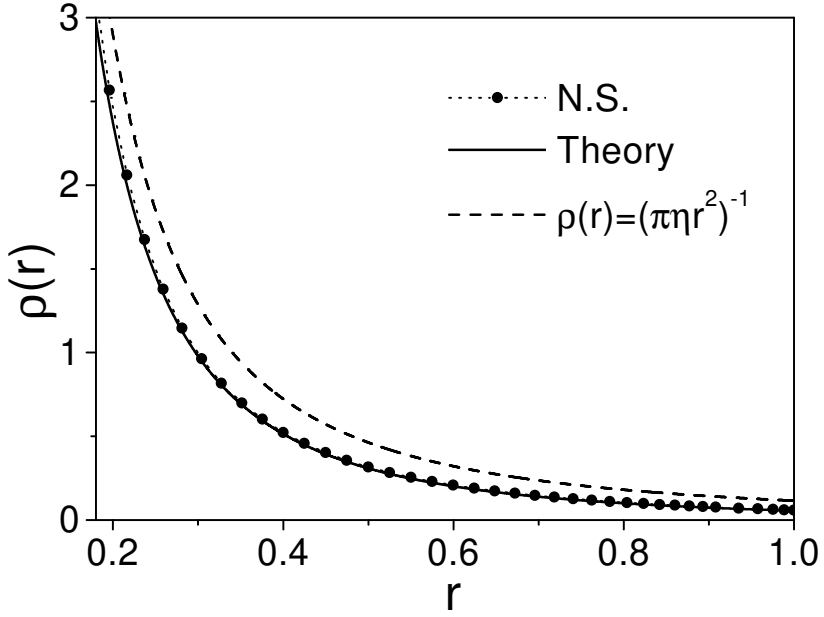


Figure 21: We plot the same numerical data (N.S.) as in Fig. 20, but in the range  $5r_0 \leq r \leq 1$ . This is compared with the theoretical density profile at  $t = t_{coll}$  obtained from Eq. (101). The parameters  $a \approx 5.0$  and  $b \approx 5.1$  are determined by maximizing  $\rho(1)$  (see text), although the full profile barely depends on  $a$  and  $b$ , as soon as  $b$  remains slightly greater than  $a$ , and  $b \approx 4.8 \sim 5.4$ . In this range, the theoretical profile is in excellent agreement with the numerical one. For instance,  $\rho(1)_{\text{N.S.}} \approx 0.058$  and  $\rho(1)_{\text{Theory}} \approx 0.057$ . In order to stress the quantitative agreement, we also plot the naive large  $r$  asymptotics of the scaling profile  $\rho_{\text{as}} = (\pi\eta r^2)^{-1}$ , for which  $\rho(1)_{\text{as}} \approx 0.116$ .

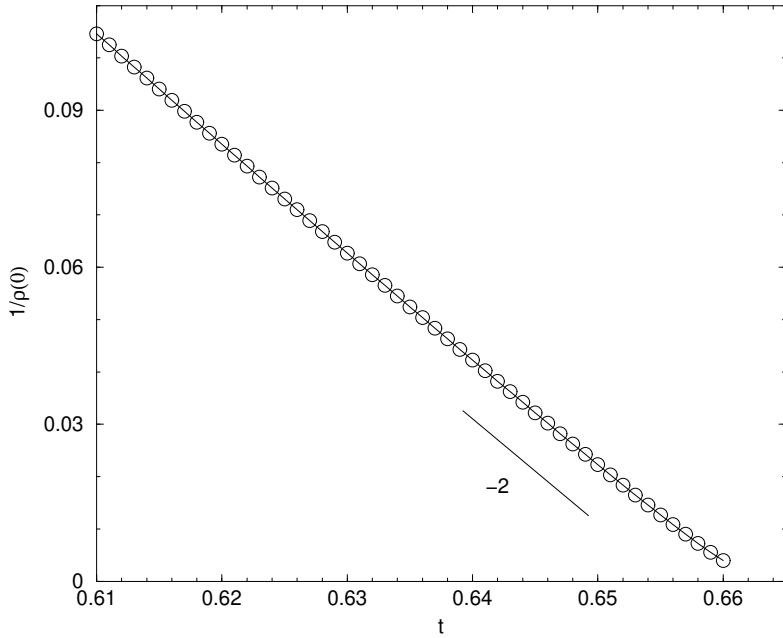


Figure 22: Evolution of the central density for  $\eta = 3.5$ . This curve displays a scaling regime  $1/\rho(0, t) = B(t_{coll} - t)$ . The slope  $B \simeq 2$  is close to the theoretical prediction  $2\pi/3 \simeq 2.1$ .

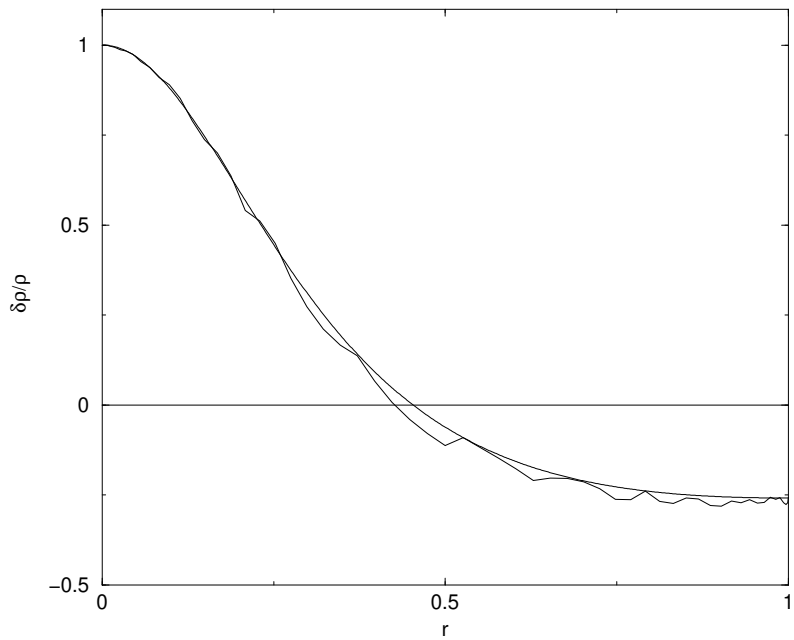


Figure 23: First mode of instability in the canonical ensemble. The density profile does not present a “core-halo” structure.

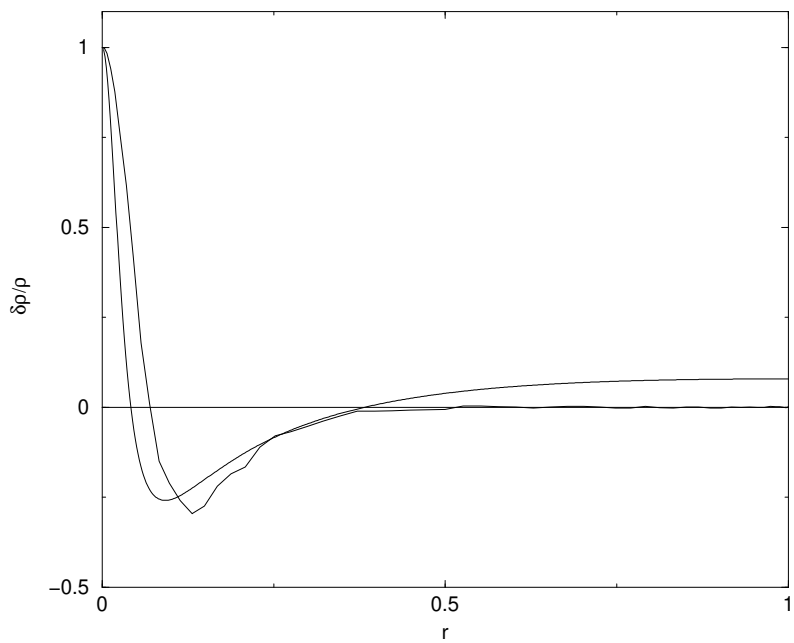


Figure 24: Second mode of instability in the canonical ensemble.

perature is fixed instead of the energy, these solutions now quickly collapse as their specific heat is negative (which is forbidden in the canonical ensemble). This clearly demonstrates that the microcanonical and canonical ensembles do not coincide for self-gravitating systems. This particular circumstance can be traced back to the non extensivity of the system due to the long range nature of the gravitational potential. This interesting problem first recognized by Lynden-Bell & Lynden-Bell [41] is discussed at length in the review paper of Padmanabhan [9].

**Result 9:** The basin of attraction of the metastable states (local entropy maxima) is non trivial.

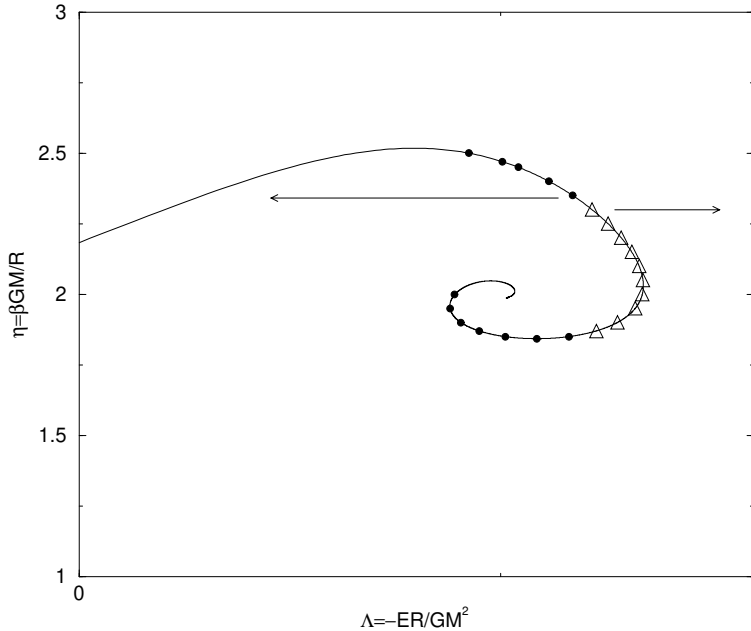


Figure 25: Bassin of attraction in the canonical ensemble.

When  $\Lambda < \Lambda_c$  in the microcanonical ensemble or  $\eta < \eta_c$  in the canonical ensemble, stable isothermal configurations exist but they are only metastable states (local entropy maxima) as discussed in section 2. Therefore, the value of the control parameter  $\Lambda$  or  $\eta$  is not sufficient to completely determine the evolution of the system: depending on its *topology*, an initial configuration can either reach a quiescent equilibrium state or develop a self-similar collapse leading to a finite time singularity. The evolution of the system depends whether this initial configuration lies in the “bassin of attraction” of the local entropy maximum or not. Of course, the complete characterization of this basin of attraction is an impossibly complicated task because we would have to consider all possible initial configurations. We have limited our study to the case where the initial state is an unstable isothermal sphere (a point on the spiral of Figs. 1-2 located after the first turning point). Even in that case, the basin of attraction is non trivial. In the canonical ensemble, this basin of attraction is displayed on Fig. 25. The isothermal spheres that undergo a complete collapse are marked with a symbol  $\Delta$  while those converging to a metastable equilibrium are marked with a symbol  $\bullet$ . It appears that the isothermal spheres undergoing isothermal collapse are located near the vertical tangent. We have found a similar diagram in the microcanonical ensemble with a concentration of points undergoing gravitational collapse located this time near the (lower) horizontal tangent. These results imply that it is possible to destabilize a metastable isothermal sphere by introducing an appropriately chosen finite amplitude perturbation. Since homogenous spheres appear to

always converge towards the metastable equilibrium state (when it exists), the destabilizing perturbation must be sufficiently concentrated. However, considering Fig. 25 again, we see that it is not the only condition since there exists highly concentrated states also converging to the metastable equilibrium state.

## 6 Conclusion

In this paper, we have discussed the thermodynamics of self-gravitating systems with the aid of a simple relaxation equation that monotonically increases entropy while conserving mass and energy. This equation provides a simplified model of “violent relaxation” by which a stellar system initially far from mechanical equilibrium tries to reach a maximum entropy state on a few dynamical times. Since a maximum entropy state does not always exist, our relaxation equation presents a rich variety of behaviors and displays interesting phase transitions between “equilibrium” and “collapsed” states. Our simple model also exhibits in a convincing way the inequivalence of ensembles for systems with long-range interactions.

We have checked the result of Antonov [12] concerning the absence of entropy maximum for  $\Lambda = -\frac{ER}{GM^2} \gtrsim 0.335$ . At this point, the system collapses and overheats in agreement with the concept of “gravothermal catastrophe” introduced by Lynden-Bell & Wood [13]. Our relaxation equation admits self-similar solutions that lead to a finite time singularity. In reality, the collapse stops when the core of the system becomes degenerate (in the sense of Lynden-Bell). In that case, the system falls on to a global entropy maximum (for the Fermi-Dirac entropy) which is the true statistical equilibrium for collisionless systems. This equilibrium state has a “core-halo” structure with a degenerate core and a dilute atmosphere. The small degenerate nucleus can contain a large mass and a variety of concentrations depending on the degeneracy parameter, as discussed in Ref. [5]. Degeneracy can be included easily in our equations [4] but we do not expect particularly new results with respect to the present study and to the equilibrium study of Ref. [5], as the mere influence of degeneracy is to put an end to the collapse.

For  $\Lambda < \Lambda_c$  there exists local entropy maxima with a smooth density profile and a density contrast  $\mathcal{R} \lesssim 709$ . Critical points of entropy with  $\mathcal{R} \gtrsim 709$  (including the singular sphere) are unstable. Depending on its *topology*, an initial condition with  $\Lambda < \Lambda_c$  can either relax towards the local entropy maximum (metastable state) or undergo a catastrophic collapse. The choice between these two behaviors clearly depends whether the initial condition lies in the “bassin of attraction” of the local entropy maximum or not. The characterization of this bassin of attraction is a difficult problem that we have illustrated only partially on some examples. It is expected [5], and corroborated by our simulations, that the bassin of attraction of the metastable equilibrium states is very wide, so that these states *are* physical. Therefore, if we introduce a repulsive potential at small distances (finite size effects or degeneracy) in order to have a global entropy maximum (corresponding to the “collapsed” state) for all values of the control parameter, the true phase transition will take place in general at the critical point  $\Lambda_c$  or  $\eta_c$  marking the *absence* of metastable equilibrium, not at the transition point  $\Lambda_t$  or  $\eta_t$  (see section 2.8) marking the passage from a global to a local equilibrium.

An extension of our study (in preparation) is to consider rotating systems with conservation of angular momentum. Our relaxation equation can be generalized easily to include angular momentum conservation (see Eq. (5.18) of Ref. [4]) and this numerical algorithm will allow us to determine maximum entropy states of rotating systems that are not spherically symmetric. Some interesting works have been done in that direction [42, 43, 44, 45], but the complete description of rotating isothermal gaseous spheres is still in its infancy stage. For some values of

the parameters the system is expected to collapse. Preliminary calculations performed within our relaxation equations indicate that the angular velocity behaves like  $\Omega(t) \sim \rho(0, t)^{1/2}$  as  $t \rightarrow t_{coll}$ , a result also obtained by Lynden-Bell [45] by considering fluid equations appropriate to the description of globular clusters.

We should finally mention that there exists an interesting analogy between stellar systems and two-dimensional vortices as discussed by one of us in a series of papers [3, 4, 10, 46, 47]. Indeed, it has been suggested that vortices in the oceans and in planetary atmospheres (e.g. Jupiter's Great Red Spot) could also be considered as maximum entropy states at fixed energy and circulation (the equivalent of mass) [48, 49, 50, 51]. Relaxation equations have been proposed in the context of 2D turbulence to describe the evolution of the flow towards a maximum entropy state [52, 4, 53, 54, 55, 56]. These relaxation equations are similar to those considered in the present article (see [4] for a precise comparison) and again lead to a Smoluchowski-Poisson system. However, the energy constraint and the space dimensionality ( $D = 2$  instead of  $D = 3$ ) are different, insuring the existence of an equilibrium state in each case. Therefore, there is no "catastrophic collapse" for 2D vortices, unlike stellar systems.

The Smoluchowski-Poisson system also appears in the description of biological systems like bacterial populations [57]. The diffusion is due to ordinary Brownian motion and the drift models a chemically directed movement (chemotactic flux) along a concentration gradient (of smell, infection, food, ...). When the attractant concentration is itself proportional to the bacterial density, this results in a coupled system morphologically similar to the one studied in the present paper. The question that naturally emerges is whether this coupling can lead to an instability for bacterial populations similar to the gravitational collapse of stellar systems. This possibility will be considered in future studies.

## 7 Acknowledgments

Preliminary results of this work were presented at the conference on Multiscale Problems in Science and Technology (Dubrovnik, Sep 2000). One of us (P.H.C.) is grateful to W. Jaeger for mentioning the connexion of this work with biological systems. This research was supported in part by the National Science Foundation under Grant No. PHY94-07194.

## A Analytical study of the scaling equation

In this Appendix, we study analytically the scaling equation (84). To that purpose, we rewrite it in an equivalent albeit more convenient form. Let us introduce the function

$$(157) \quad g(x) = \frac{1}{x^2} \int_0^x f(x') x'^2 dx',$$

in terms of which Eq. (84) becomes

$$(158) \quad f(x) + \frac{x}{\alpha} f'(x) = \frac{1}{x^2} \frac{d}{dx} \{x^2 (f'(x) + 4\pi f(x)g(x))\}$$

or, equivalently,

$$(159) \quad f(x) + \frac{x}{\alpha} f'(x) = f''(x) + \frac{2}{x} f'(x) + 4\pi (f'(x)g(x) + f^2(x)).$$

Multiplying both sides of equation (158) by  $x^2$  and integrating the resulting expression between 0 and  $x$ , we obtain

$$(160) \quad g(x) = \frac{xf(x) - \alpha f'(x)}{3 - \alpha + 4\pi\alpha f(x)}.$$

If we insert this expression for  $g(x)$  back into Eq. (159), we find that  $f$  satisfies a second-order differential equation instead of the initial third order integrodifferential equation (159). Indeed,

$$(161) \quad f''(x) + f'(x) \left( \frac{2}{x} - \frac{(3/\alpha - 1)x + 4\pi\alpha f'(x)}{3 - \alpha + 4\pi\alpha f(x)} \right) + 4\pi f^2(x) - f(x) = 0.$$

From Eqs. (157)-(160), one can derive a nonlinear recursion relation satisfied by the coefficients  $a_n$  of the series expansion of  $f(x)$  in powers of  $x^2$  (as  $f$  is an even function). Writing

$$(162) \quad f(x) = \frac{1}{4\pi} \sum_{n=0}^{+\infty} (-1)^n a_n x^{2n},$$

we find

$$(163) \quad a_{n+1} = -\frac{2n + \alpha}{2\alpha(n+1)(2n+3)} a_n + \frac{1}{2(n+1)} \sum_{p=0}^n \frac{a_p a_{n-p}}{2p+3}.$$

This recursion relation leads to the large  $n$  behavior of  $a_n$ :

$$(164) \quad a_n \sim 8r \left( n + \frac{3}{2} \right) r^n + o(r^n),$$

where  $r$  is an unknown constant related to the inverse radius of convergence of the series. For  $\alpha = 2$ , the asymptotics given by Eq. (164) with  $r = 1/2$  is an *exact* solution of the recursion relation (163). Then the series (162) can easily be resummed leading to Eq. (90).

## B The case of cold systems ( $T = 0$ )

In this Appendix, we solve Eq. (56) analytically for  $T = 0$ . Since the diffusion term vanishes, this equation describes in fact a *deterministic* motion where the particules have a velocity

$$(165) \quad \mathbf{u} = -\frac{1}{\xi} \nabla \Phi$$

directly proportional to the gravitational force (see section 3.1). This deterministic problem can be solved exactly by adapting the procedure followed by Penston [40] in his investigation of the collapse of cold self-gravitating gaseous spheres.

Let us consider a particle located at  $r(0) = a$  at time  $t = 0$ . We denote by  $\bar{\rho}(a)$  the average density inside radius  $a$ . The total mass inside radius  $a$  can therefore be expressed as

$$(166) \quad M_a = \frac{4\pi}{3} \bar{\rho}(a) a^3.$$

A time  $t$  this mass is now contained in the sphere of radius  $r(t) = r$ , where  $r(t)$  is the position of the particule initially at  $r = a$ . According to equation (165) and the Gauss theorem (61), the motion of the particle is described by the first order differential equation

$$(167) \quad \frac{dr}{dt} = -\frac{1}{\xi} \frac{GM_a}{r^2}.$$

This equation can be integrated explicitly to give

$$(168) \quad r = a \left( 1 - \frac{4\pi G}{\xi} \bar{\rho}(a) t \right)^{1/3}.$$

Let us first discuss the case where the system is initially homogeneous with density  $\bar{\rho}(a) = \bar{\rho}_0$ . In that case, all the particles (whatever their initial position) arrive at  $r = 0$  at a time

$$(169) \quad t_{coll} = \frac{\xi}{4\pi G \bar{\rho}_0},$$

defined as the collapse time for  $T = 0$ . This expression represents a lower bound on the value of the collapse time  $t_{coll}(\eta)$  studied in section 4.4. Note that during all the evolution, the sphere remains homogeneous with radius, density and free energy evolving as

$$(170) \quad R(t) = R(1 - t/t_{coll})^{1/3}, \quad \rho(t) = \bar{\rho}_0(1 - t/t_{coll})^{-1},$$

$$(171) \quad J(t) \sim \frac{3\beta GM^2}{5R(t)} = \frac{3\beta GM^2}{5R} (1 - t/t_{coll})^{-1/3}.$$

These results can also be obtained directly from Eq. (56) which reduces, for a uniform density, to

$$(172) \quad \frac{d\rho}{dt} = \nabla \left( \frac{1}{\xi} \rho \nabla \Phi \right) = \frac{1}{\xi} \rho \Delta \Phi = \frac{4\pi G}{\xi} \rho^2,$$

where we have used the Poisson equation (4) to get the last equality. This argument shows that the solution (170)(171) is still a particular solution of the problem when  $T \neq 0$ . However, it may not be stable when a diffusion term is present in the equation.

We now suppose that, initially,  $\bar{\rho}(a)$  has a smooth maximum at the center so that

$$(173) \quad \bar{\rho}(a) = \bar{\rho}_0 \left(1 - \frac{a^2}{A^2}\right),$$

for sufficiently small  $a$ , where  $A$  is a constant. In that case, Eq. (168) giving the position at time  $t$  of the particle located at  $r = a$  at  $t = 0$  becomes

$$(174) \quad r = a \left[1 - \left(1 - \frac{a^2}{A^2}\right) \frac{t}{t_{coll}}\right]^{1/3}.$$

At  $t = t_{coll}$ , the time at which the central density becomes infinite, it reduces to

$$(175) \quad r = \frac{a^{5/3}}{A^{2/3}}.$$

It is now straightforward to obtain the full density profile at  $t = t_{coll}$ . Since the mass contained between  $a$  and  $a + da$  at  $t = 0$  arrives between  $r$  and  $r + dr$  at time  $t$ , we have in full generality

$$(176) \quad \bar{\rho}(a) 4\pi a^2 da = \rho(r, t) 4\pi r^2 dr,$$

or, for sufficiently small  $a$ ,

$$(177) \quad \rho(r, t) = \bar{\rho}(a) \frac{a^2}{r^2} \frac{da}{dr} \simeq \bar{\rho}_0 \frac{a^2}{r^2} \frac{da}{dr}.$$

Now, using Eqs. (177)-(175) at  $t = t_{coll}$ , we get

$$(178) \quad \rho(r, t_{coll}) = \frac{3}{5} \bar{\rho}_0 A^{6/5} r^{-6/5}.$$

We have therefore established that, for  $T = 0$ , the density profile decreases algebraically with an exponent  $\alpha = 6/5$ .

We now extend this analysis to a time  $\tau = t_{coll} - t$  just before the singularity arises. Considering the limit  $a \rightarrow 0$  and  $\tau \rightarrow 0$ , Eq. (174) can be expanded to lowest order as

$$(179) \quad r = a \left( \frac{\tau}{t_{coll}} + \frac{a^2}{A^2} \right)^{1/3}.$$

Then, Eq. (177) leads, after some reductions, to the density profile

$$(180) \quad \rho(r, t) = \frac{\bar{\rho}_0}{\frac{\tau}{t_{coll}} + \frac{5a^2}{3A^2}}.$$

The central density corresponds to  $r = 0$ , i.e.  $a = 0$ . According to Eq. (180) it evolves with time as

$$(181) \quad \rho(0, t) = \frac{\bar{\rho}_0 t_{coll}}{\tau} = \frac{\xi}{4\pi G} (t_{coll} - t)^{-1}.$$

Therefore, if we define

$$(182) \quad s = \frac{5a^2 t_{coll}}{3A^2 \tau},$$

we can express the scaled density as:

$$(183) \quad \frac{\rho(r, t)}{\rho(0, t)} = \frac{1}{1+s}.$$

On the other hand, the relation (179) between  $r$  and  $a$  can be written

$$(184) \quad \frac{r}{\bar{r}_0(t)} = s^{1/2} \left(1 + \frac{3}{5}s\right)^{1/3},$$

where we have defined the “core radius” by

$$(185) \quad \bar{r}_0 = \left(\frac{3A^2}{5}\right)^{1/2} \left(\frac{\tau}{t_{coll}}\right)^{5/6}.$$

According to Eq. (181) and (185), we have the scaling laws

$$(186) \quad \bar{r}_0 \sim (t_{coll} - t)^{5/6}, \quad \rho(0)\bar{r}_0^{6/5} \sim 1,$$

just before the singularity occurs. In addition, Eqs. (183)-(184) determine the invariant profile  $F(x)$  in a parametric form (here,  $F = \rho/\rho(0)$  and  $x = r/\bar{r}_0$ ). We can easily check that

$$(187) \quad F(x) = 1 - x^2 + \dots \quad (x \rightarrow 0),$$

$$(188) \quad F(x) \sim \left(\frac{3}{5}\right)^{2/5} x^{-6/5} \quad (x \rightarrow +\infty).$$

This solves the problem for  $T = 0$ . Now, if the temperature  $T$  is very small but non-zero, we expect the present scaling to hold provided that  $\bar{r}_0 \gg r_0(t)$ , where  $r_0$  is defined in section 4. This leads to a cross-over core density  $\rho_0^*$  above which the  $T \neq 0$  scaling of section 4.2 will prevail. The density  $\rho_0^*$  can be estimated by equating  $r_0 = (T/G\rho_0)^{1/2}$  to  $\bar{r}_0 \sim \rho_0^{-5/6}$ . The  $T \neq 0$  scaling then prevails when the density becomes high enough:

$$(189) \quad \rho_0^* \sim \left(\frac{T}{G}\right)^{-3/2}.$$

For those who prefer a more mathematical proof of these results, we look for self-similar solutions of Eq. (56), with  $T = 0$ , following the methods of section 4. In the present context, the core radius is not given by the King radius (78) which is zero by definition. We still assume however that  $\rho_0 \bar{r}_0^\alpha \sim 1$ , where  $\alpha$  is unknown *a priori*. The equation for the invariant profile is then given by

$$(190) \quad f(x) + \frac{x}{\alpha} f'(x) = \frac{1}{x^2} \frac{d}{dx} (4\pi x^2 f(x) g(x)),$$

where  $g(x)$  is defined by Eq. (157). An equivalent form of Eq. (190) is

$$(191) \quad f(x) + \frac{x}{\alpha} f'(x) = 4\pi (f'(x) g(x) + f^2(x)).$$

Multiplying Eq. (190) by  $x^2$  and integrating from 0 to  $x$  we obtain

$$(192) \quad g(x) = \frac{x f(x)}{3 - \alpha + 4\pi \alpha f(x)}.$$

Substituting the foregoing expression for  $g(x)$  in Eq. (191), we find that  $f(x)$  satisfies the first order nonlinear differential equation

$$(193) \quad -\frac{(3/\alpha - 1)x}{3 - \alpha + 4\pi\alpha f(x)} f'(x) + 4\pi f^2(x) - f(x) = 0.$$

Expanding  $f(x)$  in Taylor series for  $x \rightarrow 0$  in Eq. (192), we get

$$(194) \quad f(0) = \frac{1}{4\pi}, \quad \alpha = \frac{6}{5},$$

which returns Eqs. (181)-(186). Considering Eq. (192) and introducing the change of variables (184) in the integral defining  $g(x)$ , we can easily check that the invariant profile  $f(x)$  defined by Eqs. (183)-(184) is solution of this equation. However, it would have been difficult to obtain this result directly from the mathematical analysis.

## C Connexion between linear stability and the second order variations of entropy

Let  $\rho$  be a stationary solution of Eq. (56) and  $\delta\rho$  a small perturbation around this solution. The first and second variations of temperature respecting the energy constraint (54) can be expressed as

$$(195) \quad \frac{3}{2}M\delta T + \int \delta\rho\Phi d^3\mathbf{r} = 0,$$

$$(196) \quad \frac{3}{2}M\delta^2T + \frac{1}{2} \int \delta\rho\delta\Phi d^3\mathbf{r} = 0.$$

The critical point  $\rho$  is a local entropy *maximum* provided that the second variations of entropy

$$(197) \quad \delta^2S = -\frac{3M}{4} \frac{(\delta T)^2}{T^2} + \frac{3M}{2} \frac{\delta^2T}{T} - \frac{1}{2} \int \frac{(\delta\rho)^2}{\rho} d^3\mathbf{r}$$

are negative for any variations that conserve mass at first order. Let us now linearize Eq. (56) around equilibrium and write the time dependance of the perturbation in the form  $\delta\rho \sim e^{\lambda t}$ . We get

$$(198) \quad \lambda\delta\rho = \nabla \left[ \frac{1}{\xi} (\delta T \nabla \rho + T \nabla \delta\rho + \delta\rho \nabla \Phi + \rho \nabla \delta\Phi) \right].$$

Multiplying both side of Eq. (198) by  $\delta\rho/\rho$ , integrating by parts and using the equilibrium condition

$$(199) \quad T \nabla \rho + \rho \nabla \Phi = 0,$$

we obtain

$$(200) \quad \lambda \int \frac{(\delta\rho)^2}{\rho} d^3\mathbf{r} = - \int \frac{1}{T\rho\xi} (T \nabla \delta\rho + \delta\rho \nabla \Phi) (\delta T \nabla \rho + T \nabla \delta\rho + \delta\rho \nabla \Phi + \rho \nabla \delta\Phi) d^3\mathbf{r}.$$

We now remark that the second order variations of the rate of entropy production (57) are given by

$$(201) \quad \delta^2 \dot{S} = \int \frac{1}{\rho T \xi} (\delta T \nabla \rho + T \nabla \delta \rho + \delta \rho \nabla \Phi + \rho \nabla \delta \Phi)^2 d^3 \mathbf{r}.$$

We can therefore rewrite Eq. (200) in the form

$$(202) \quad \begin{aligned} \lambda \int \frac{(\delta \rho)^2}{\rho} d^3 \mathbf{r} = -\delta^2 \dot{S} + \int \frac{1}{T \rho \xi} & (\delta T \nabla \rho + \rho \nabla \delta \Phi) \\ & \times (\delta T \nabla \rho + T \nabla \delta \rho + \delta \rho \nabla \Phi + \rho \nabla \delta \Phi) d^3 \mathbf{r}. \end{aligned}$$

Using Eq. (199), the last term in Eq. (202) is clearly the same as

$$(203) \quad - \int \frac{1}{\xi} (\delta T \nabla \rho + T \nabla \delta \rho + \delta \rho \nabla \Phi + \rho \nabla \delta \Phi) \left( \frac{\delta T}{T^2} \nabla \Phi - \frac{1}{T} \nabla \delta \Phi \right) d^3 \mathbf{r}.$$

Taking the time derivative of Eq. (54) and using Eq. (56) we have at each time

$$(204) \quad \dot{E} = \frac{3}{2} M \dot{T} - \int \frac{1}{\xi} (T \nabla \rho + \rho \nabla \Phi) \nabla \Phi d^3 \mathbf{r} = 0.$$

The energy constraint (204) must be satisfied to first and second order. This yields:

$$(205) \quad \int \frac{1}{\xi} (\delta T \nabla \rho + T \nabla \delta \rho + \delta \rho \nabla \Phi + \rho \nabla \delta \Phi) \nabla \Phi d^3 \mathbf{r} = \frac{3}{2} M \delta \dot{T} = \frac{3}{2} M \lambda \delta T,$$

$$(206) \quad \int \frac{1}{\xi} (\delta T \nabla \rho + T \nabla \delta \rho + \delta \rho \nabla \Phi + \rho \nabla \delta \Phi) \nabla \delta \Phi d^3 \mathbf{r} = \frac{3}{2} M \delta^2 \dot{T} = 3 M \lambda \delta^2 T,$$

where we have used Eqs. (195)-(196) to obtain the last equalities. Substituting these relations in Eq. (202), we get

$$(207) \quad \lambda \left\{ \int \frac{(\delta \rho)^2}{\rho} d^3 \mathbf{r} + \frac{3M}{2} \frac{(\delta T)^2}{T^2} - 3M \frac{\delta^2 T}{T} \right\} = -\delta^2 \dot{S}.$$

Comparing with Eq. (197), we finally obtain

$$(208) \quad \delta^2 \dot{S} = 2\lambda \delta^2 S.$$

Since  $\delta^2 \dot{S} \geq 0$ , see Eq. (201), the sign of  $\lambda$  is the same as that of  $\delta^2 S$ . If  $\rho$  is a local entropy maximum, then  $\delta^2 S < 0$  and  $\lambda < 0$  for any perturbation: the solution is linearly stable. Otherwise, we can find a perturbation for which  $\delta^2 S$ , and consequently  $\lambda$ , are positive: the solution is linearly unstable. We can easily extend the relation (208) in the canonical ensemble with  $J$  instead of  $S$ . We have found the same relation for other kinetic equations (Chavanis, in preparation), so its validity seems to be of a very wide scope.

## References

- [1] J. Binney and S. Tremaine, *Galactic Dynamics* (Princeton Series in Astrophysics, 1987).
- [2] D. Lynden-Bell, “Statistical mechanics of violent relaxation in stellar systems”, Mon. Not. R. astr. Soc. **136**, 101 (1967).

- [3] P.H. Chavanis, Contribution à la mécanique statistique des tourbillons bidimensionnels. Analogie avec la relaxation violente des systèmes stellaires, Thèse de doctorat, Ecole Normale Supérieure de Lyon (1996).
- [4] P.H. Chavanis, J. Sommeria and R. Robert, “Statistical mechanics of two-dimensional vortices and collisionless stellar systems”, *Astrophys. J.* **471**, 385 (1996).
- [5] P.H. Chavanis and J. Sommeria, “Degenerate equilibrium states of collisionless stellar systems”, *Mon. Not. R. astr. Soc.* **296**, 569 (1998).
- [6] P.H. Chavanis “On the coarse-grained evolution of collisionless stellar systems”, *Mon. Not. R. astr. Soc.* **300**, 981 (1998).
- [7] P.H. Chavanis, “Statistical mechanics of violent relaxation in stellar systems”, to appear in the Proceedings of the Conference on Multiscale Problems in Science and Technology (Springer, 2001).
- [8] H.E. Kandrup, “Stochastic gravitational fluctuations in a self-consistent mean field theory”, *Physics Reports* **63**, 1 (1980).
- [9] T. Padmanabhan, “Statistical mechanics of gravitating systems”, *Phys. Rep.* **188**, 285 (1990).
- [10] P.H. Chavanis, “From Jupiter’s great red spot to the structure of galaxies: statistical mechanics of two-dimensional vortices and stellar systems”, *Annals of the New York Academy of Sciences* **867**, 120 (1998).
- [11] S. Chandrasekhar, *An Introduction to the Theory of Stellar Structure* (Dover 1942).
- [12] V.A. Antonov, *Vest. Leningr. Gos. Univ.* **7**, 135 (1962).
- [13] D. Lynden-Bell and R. Wood, “The gravothermal catastrophe in isothermal spheres and the onset of red-giants structure for stellar systems”, *Mon. Not. R. astr. Soc.* **138**, 495 (1968).
- [14] S. Inagaki and D. Lynden-Bell, “Self-similar solutions for post-collapse evolution of globular clusters”, *Mon. Not. R. astr. Soc.* **205**, 913 (1983).
- [15] E. Bettwieser and D. Sugimoto, “Post-collapse evolution and gravothermal oscillation of globular clusters”, *Mon. Not. R. astr. Soc.* **208**, 493 (1984).
- [16] C. Rosier, “Problème de Cauchy pour une équation parabolique modélisant la relaxation des systèmes stellaires auto-gravitants”, to appear in *C. R. Acad. Sci. Paris, Série I*.
- [17] T. Padmanabhan, “Antonov instability and the gravothermal catastrophe-revisited”, *Astrophys. J. Supp.* **71**, 651 (1989).
- [18] P.H. Chavanis, “Gravitational instability of finite isothermal spheres”, submitted to *Astron. Astrophys.* [astro-ph/0103159].
- [19] R. Robert, “On the gravitational collapse of stellar systems”, *Class. Quantum Grav.* **15**, 3827 (1998).
- [20] R.W. Michie, “On the distribution of high energy stars in spherical stellar systems”, *Mon. Not. R. Astr. Soc.* **125**, 127 (1963).

- [21] I.R. King, “The structure of star clusters. II. Steady-state velocity distribution”, *Astron. J.* **70**, 376 (1965).
- [22] J. Katz, “On the number of unstable modes of an equilibrium”, *Mon. Not. R. astr. Soc.* **183**, 765 (1978).
- [23] H.J. de Vega and N. Sanchez, “Statistical mechanics of the self-gravitating gas: I. Thermodynamical limit and phase diagrams”, [astro-ph/0101567].
- [24] R.B. Larson, “A method for computing the evolution of star clusters”, *Mon. Not. R. astr. Soc.* **147**, 323 (1970).
- [25] H. Cohn, “Late core collapse in star clusters and the gravothermal instability”, *Astrophys. J.* **242**, 765 (1980).
- [26] D. Lynden-Bell and P.P. Eggleton, “On the consequences of the gravothermal catastrophe”, *Mon. Not. R. astr. Soc.* **191**, 483 (1980).
- [27] S.L. Shapiro and S.A. Teukolsky, “The collapse of dense star clusters to supermassive black hole: the origin of quasars and AGNs”, *Astrophys. J.* **292**, L41 (1995).
- [28] J. Katz, “Stability limits for isothermal cores in globular clusters”, *Mon. Not. R. astr. Soc.* **190**, 497 (1980).
- [29] G. Ingrosso, M. Merafina, R. Ruffini and F. Strafella, “System of self-gravitating semidegenerate fermions with a cutoff of energy and angular momentum in their distribution function”, *Astron. Astrophys.* **258**, 223 (1992).
- [30] B.B. Kadomtsev and O.P. Pogutse, “Collisionless relaxation in systems with Coulomb interactions”, *Phys. Rev. Lett.* **25**, 1155 (1970).
- [31] G. Severne and M. Luwel, “Dynamical theory of collisionless relaxation”, *Astrophys. & Space Sci.* **72**, 293 (1980).
- [32] E. Follana and V. Laliena, “Thermodynamics of self-gravitating systems with softened potentials”, *Phys. Rev. E* **61**, 6270 (2000).
- [33] F. Leeuwin and E. Athanassoula, “Central cusp caused by a supermassive black hole in axisymmetric models of elliptical galaxies”, *Mon. Not. R. astr. Soc.* **417**, 79 (2000).
- [34] M. Stiavelli, “Violent relaxation around a massive black hole”, *Astrophys. J. Lett.* **495**, L91 (1998).
- [35] A. Kull, R.A. Treumann and H. Böringer, “Violent relaxation of indistinguishable objects and neutrino hot dark matter in clusters of galaxies”, *Astrophys. J. Lett.* **466**, L1 (1996).
- [36] J. Hjorth and J. Madsen, “Violent relaxation and the  $R^{1/4}$  law”, *Mon. Not. R. Astr. Soc.* **253**, 703 (1991).
- [37] M. Stiavelli and G. Bertin, “Statistical mechanics and equilibrium sequences of ellipticals”, *Mon. Not. R. astr. Soc.* **229**, 61 (1987).
- [38] S. Chandrasekhar, “Stochastic problems in physics and astronomy”, *Reviews of Modern Physics* **15**, 1 (1943).

- [39] H. Risken, *The Fokker-Planck equation* (Springer, 1996).
- [40] M.V. Penston, “Dynamics of self-gravitating gaseous spheres-III. Analytical results in the free-fall of isothermal cases.”, *Mon. Not. R. astr. Soc.* **144**, 425 (1969).
- [41] D. Lynden-Bell and R. Lynden-Bell, “On the negative specific heat paradox”, *Mon. Not. R. astr. Soc.* **181**, 405 (1977).
- [42] C. Lagoute and P.Y. Longaretti, “Rotating globular clusters. I. Onset of the gravothermal instability.”, *Astron. Astrophys.* **308**, 441 (1996).
- [43] V. Laliena, “Effect of angular momentum conservation in the phase transition of collapsing systems”, *Phys. Rev. E* **59**, 4786 (1999).
- [44] O. Fliegans and D.H.E. Gross, “Effect of angular momentum on equilibrium properties of a self-gravitating system”, submitted to *Phys. Rev. E*. (2001) [cond-mat/0102062].
- [45] D. Lynden-Bell, “Rotation, statistical dynamics and kinematics of globular clusters”, [astro-ph/0007116].
- [46] P.H. Chavanis and C. Sire, “Statistics of velocity fluctuations arising from a random distribution of point vortices: The speed of fluctuations and the diffusion coefficient”, *Phys. Rev. E* **62**, 490 (2000).
- [47] P.H. Chavanis, “On the analogy between two-dimensional vortices and stellar systems”, Proceedings of the IUTAM Symposium on Geometry and Statistics of Turbulence (2001), T. Kambe, T. Nakano and T. Miyauchi Eds. (Kluwer Academic Publishers).
- [48] L. Onsager, “Statistical hydrodynamics”, *Nuovo Cimento Suppl.* **6**, 279 (1949).
- [49] G. Joyce and D. Montgomery, “Negative temperature states for the two-dimensional guiding-center plasma”, *J. Plasma Physics* **10**, 107 (1973).
- [50] J. Miller, “Statistical mechanics of the Euler equation in two dimensions”, *Phys. Rev. Lett.* **65**, 2137 (1990).
- [51] R. Robert and J. Sommeria, “Statistical equilibrium states for two-dimensional flows”, *J. Fluid. Mech.* **229**, 291 (1991).
- [52] R. Robert and J. Sommeria, “Relaxation towards a statistical equilibrium state in two-dimensional perfect fluid dynamics”, *Phys. Rev. Lett.* **69**, 2776 (1992).
- [53] R. Robert and C. Rosier, “The modelling of small scales in 2D turbulent flows: a statistical mechanics approach”, *J. Stat. Phys.* **86**, 481 (1997).
- [54] P.H. Chavanis “Systematic drift experienced by a point vortex in two-dimensional turbulence”, *Phys. Rev. E* **58**, R1199 (1998).
- [55] P.H. Chavanis “Quasilinear theory of the 2D Euler equation”, *Phys. Rev. Lett.* **84**, 5512 (2000).
- [56] P.H. Chavanis “Kinetic theory of point vortices: diffusion coefficient and systematic drift”, to appear in *Phys. Rev. E* (2001) [cond-mat/0107219].
- [57] J.D. Murray, *Mathematical Biology* (Springer, 1991).